Journal of Mathematical Techniques in Modeling; Vol.1, Issue.1, 2024
https://doi.org/10.56868/jmtm.v1i1.3

Research Paper https://www.ufpub.com/index.php/jmtm/index

Navigating Food Allergy Dynamics via a Novel Fractional Mathematical Model for Antacid-Induced Allergies

Wajahat Ali Khan[1], **Rahat Zarin**[2,†*], **Aurang Zeb**[3], **Yousaf Khan**[3], **Amir Khan** [3]
[1]Department of Mathematics, University of Malakand, Chakdara, Pakistan
[2]Department of Mathematics, Faculty of Science, King Mongkut's University of Technology, Thonburi (KMUTT), Bang Mod Thrung Khru, Bangkok 10140, Thailand
[3] Department of Mathematics and Statistics, University of Swat, Khyber Pakhtunkhawa, Pakistan

ABSTRACT

This study explores the onset of food allergies in individuals using antacid medications, employing an innovative fractional mathematical model integrating fractional calculus and differential equations. Through this methodology, we analyze the intricate dynamics of food allergy epidemics and their interaction with antacid usage, offering essential perspectives for refining management strategies and implementing early intervention measures. Our research stems from a 2001 case, marking the initial occurrence of a severe anaphylactic reaction to manioc, a novel food allergy. Prompted by the prolonged acknowledgment of incidents involving a tuber ingrained in native Brazilians' diets for over 500 years, we establish a mathematical framework addressing the persistence of the cassava allergen in the presence of proton pump inhibitors (PPIs). These medications, utilized to reduce gastric acidity in digestive disorders, elevate pH levels, fostering the preservation of the allergen and subsequently enhancing immune recognition. Our investigation hinges on employing a mathematical model to scrutinize how incidents related to food allergies impact the dynamics of scientific publication. The model, offering a distinctive perspective on food allergy characterization, relies on a novel set of differential equations incorporating fractional Caputo-Fabrizio (CF) operators. Insights into the model's long-term behavior are derived from a comprehensive examination of its qualitative characteristics and subsequent computational simulations. We establish the existence and uniqueness of solutions within the proposed model, drawing on established results concerning fixed points. Utilizing the Ulam-Hyers method, we determine stability outcomes. For in-depth numerical analysis and simulation, our study employs Newton's polynomial in conjunction with the three-step Adams-Bashforth numerical technique. The findings underscore the efficacy of fractional order techniques in accurately capturing the complex dynamics of food allergies and providing insightful information crucial for devising effective management plans.

Keywords: Food Allergy, Stability Analysis, Three-step Adams-Bashforth, Newton's Polynomial, Fractional Modeling, Numerical Simulations

*Corresponding author: rahatmathematicion@gmail.com
Received: October 8, 2023; **Received in the revised form:** October 23, 2023; **Accepted:** December 05, 2023
Available online: January 06, 2024

1 Introduction

An allergic reaction to manioc, also known as cassava or tapioca, was documented by Chiron et al. [1] in 2001, establishing the first case of a novel food allergy. The first instance of cross-reactivity between cassava and natural rubber latex was discovered almost simultaneously by Galvo et al. [2], a phenomenon that was further discussed by a collaborative team from Portugal [3]. Ibero et al. [4] described a different case. Manihot esculenta, also known as Manihot utilissima, refers to this carbohydrate-rich tuberous source that is widely consumed in Brazil and more than 80 other nations, mostly in South America, Asia, and Africa. Given that indigenous populations have consumed this dietary staple for well over 500 years, prior to the country's discovery, it begs the puzzling question as to why the first cases of such allergies are only now manifesting in Brazil. Although a cursory explanation of an incomplete diagnosis might be given, this claim is tenuous given the long-standing availability of specialised knowledge and the technical requirements for complete allergy diagnostics. The discovery of immunoglobulin E (IgE) [5] has significantly advanced allergy diagnostics in recent years.

Additionally, the field of medical literature had previously engaged with clinical data prior to the establishment of specialised methodologies, giving medical professionals the ability to recognise and diagnose emerging allergic phenomena. It is therefore clear that the emergence of cassava allergies represents a recent worry. The assumption that one or more factors may have contributed to the onset of sensitisation and allergic reactions arises from the population's prolonged exposure to this dietary component over time. To better understand this issue, our research project included a thorough investigation ranging from clinical studies to molecular biology. In the course of this investigation, we identified a previously unidentified allergen known as Man e 5, which shows cross-reactivity with Hev b 5 found in natural rubber latex [6].

Going back to the original question, the recent increase in the prevalence of this allergy raises concerns about causality. As explained in reference [7], the growing use of proton pump inhibitors (PPIs) to treat gastrointestinal disorders has been taken into consideration. Since its inception in 1988, this therapeutic category has expanded significantly around the world, with Brazil playing a significant role in adoption. The HC-USP group's investigations into this recently discovered allergen have revealed its relationship to a particular subset of proteins known as "natively unfolded" or "intrinsically unstructured," as shown in reference [8]. According to empirical observations, proteins in this class do not exhibit ordered structural conformation or are predicted to do so [9]. These proteins have an exceptional susceptibility to pepsin's enzymatic activity in the acidic environment of gastric juices as a result of these innate qualities, which causes their rapid degradation within seconds (unpublished data). The development of "leaky gut syndrome" as a result of taking antacid medications, particularly PPIs, makes it easier for food to not fully break down, which allows for early nutrient absorption [10, 11]. According to the literature, this phenomenon is linked to immunological fatigue and the potential emergence of food allergies. In this situation, the elevated pH levels associated with PPI use preserve the structural integrity of the cassava allergen, making it easier for the immune system to identify.

The question arising from the empirical data mentioned above relates to the identification of a cassava allergy in the Brazilian population in 2002, which was a time after the introduction of PPIs in 1988. A thorough analysis is required in order to respond to this question. Between the beginning of a new pharmaceutical product's introduction to the market and the ensuing exponential growth in its utilisation, there is inherently a time lag. A factor adding to the complexity of the situation is the introduction of novel agents with comparable effects into the pharmaceutical landscape. Additionally, it is important to take into account the diversity of drug use patterns; a portion of the population exhibits sporadic and indiscriminate drug use, which is accompanied by a genetic susceptibility to sensitisation. Along with the time between the onset of allergic symptoms and a formal diagnosis, another consideration is the temporal progression required for the body to become sensitised to a new allergen. Determining the answer to this complex question depends critically on a thorough

understanding of these complex factors.

Lately, a profusion of mathematical models has emerged within the domain of fractional calculus, showcasing remarkable efficacy in resolving diverse real-world challenges, a feat attributed to the incorporation of initial conditions. As a result, this topic has received a lot of attention in recent discourse. This sharpened focus is evident in a variety of contexts [12–19]. Fractional calculus (FC)'s theoretical underpinnings and real-world applications have been the subject of growing international intrigue. This increase in interest is primarily attributable to fractional calculus' broad applicability across a range of fields in biology, engineering, and the physical sciences, including physics, chemistry, algebra, epidemiology, optics, ecological systems, and more. The fundamental tool for better understanding the inherent complexity of natural phenomena is fractional calculus. As a result, fractional calculus has the potential to have a big impact on the field of environmental analysis and comprehension. The creation of novel fractional operators with distinguishing features is essential to the simulation of genuine real-world puzzles. In the field of fractional calculus, researchers have focused on developing and using novel fractional operators that have applications in a variety of situations [20–22]. Fractional derivatives have the potential to be used to model systems whose dynamics are affected by memories of earlier states because of their non-local nature. The flexibility to select the fractional order that best aligns with empirical data bestows the model with the capability to be finely calibrated to factual observations, thereby facilitating enhanced comprehension of disease progression mechanisms.

The following sections of this manuscript are arranged in a methodical manner as follows: The formulation and presentation of the fractional-order model of friction are the focus of Section 2. In Section 3 the basic characteristics inherent to the foundational model are discussed. The subsequent Section 4 presents a thorough theoretical analysis of the fractional model, including enquiries into its existence, singularity, and stability traits. Moving on, Section 5 describes the numerical approach taken to arrive at the system's numerical solution and imparts profound insights into the influence of various parameters through the visualisation of graphs. The study comes to a close in Section 6, which offers useful insights into the dynamical aspects of the epidemic food allergy phenomenon.

2 Formulation of the model

A mathematical framework is created by imposing specific assumptions to compare the individual manifestation of such allergies with the prevalence of food allergies within a community [23]. Despite cassava being a common food source for allergies, conventional wisdom assumed there were no antacid interventions by the pharmaceutical industry prior to their introduction. The variable $\mathcal{P}$ represents the percentage of people at time t who have never previously developed an allergy to the allergen. The introduction of antacid medication then takes place among a completely ignorant demographic. The number of people using antacid treatments, denoted by $\mathcal{U}$, gradually increases over time in accordance with industry investments in advertising campaigns and the effectiveness of the antacid formulation. However, due to a variety of factors, including regulatory requirements, decreased adherence among the population who are not sensitised, and production capacity restrictions for pharmaceuticals, this growth eventually reaches saturation. The hypothesis, expressed as $(\sim \alpha P$, for $U > 1)$, is based on the idea that the influx of new antacid users exhibits an inverse correlation with both the population of non-sensitized individuals and the existing antacid users. These qualities are combined in this conceptualisation. As mentioned in [24], this dynamic has been used before in the context of cancer cell drug uptake. The parameter α, also known as the recruitment rate, encompasses a variety of dynamics, including the impact of marketing tactics that target susceptible people (P) and user recommendations $(\mathcal{U})$, and it ultimately determines how often people take their antacids. With a small cohort of antacid users $(\sim \alpha P$, for $U > 1)$, a discernible transition is seen.While an increase in user numbers causes recruitment to reach saturation $(\sim \alpha \mathcal{P}\mathcal{U}/\mathcal{K}$, for $\mathcal{U} \sim 0)$ [25]. Lower value situations quickly reveal the influence of saturation, overshadowing the function of mass action kinetics. The scaling factor controlling the hiring process is the parameter $\mathcal{K}_{\mathcal{P}}$.

Antiacid users develop immune sensitisation as a result of residual micro-proteins, including food allergens, in the gastric milieu that are then taken up by epithelial cells. The concentration of food allergens [26] available for interaction with antigen-presenting cells (APCs) intricately determines the extent of this sensitisation. There is typically a threshold for allergen concentrations that defines the range necessary for effective immune cell sensitisation. The population-level sensitisation process, parameterized by the term $\beta\mathcal{U}^2/\left(\mathcal{K}_{\mathcal{U}}^2+\mathcal{U}^2\right)$, finds an analogue for these microbiological dynamics. In this formulation, β denotes the rate of sensitisation for antiacid users, converting them into the sensitised subgroup denoted as S, which represents the number of sensitised people at time t. Sensitisation symptoms are more noticeable at lower antiacid usage levels $\left(\sim \beta\mathcal{U}^2/\mathcal{K}_{\mathcal{U}}^2\text{, for } \mathcal{U}\propto\mathcal{K}_{\mathcal{U}}^2\right)$; however, as the user population grows, the occurrence of sensitisation becomes saturated $(\sim \beta\text{, for } \mathcal{U}>1)$. The existence of a threshold concentration of food allergens necessary for sensitisation gives rise to this saturation phenomenon. The scaling coefficient for the parameter $\mathcal{K}_v$ that controls the sensitisation procedure emerges. Some members of the sensitised cohort are predisposed to developing an immune reaction against food allergens as a result of genetic predispositions and environmental factors. The term $\gamma S^3/\left(\mathcal{K}_s^3+\mathcal{S}^3\right)$, where γ stands for the rate of allergic response acquisition among sensitised individuals, describes this event, which is less common than sensitisation. As a result of this process, these people are moved into the $\mathcal{A}$ category of food allergic people, which represents the total number of food-allergic people at time t. Similar to sensitisation, the development of food allergies shows a muted propensity in individuals with lower levels of sensitisation $(\sim\gamma\text{, for } \mathcal{S}\times 1)$ Saturation is visible with an increase in the sensitised population $\left(\sim\gamma S^3/\mathcal{K}_{\mathcal{S}}^3\text{, for } \mathcal{S}\propto\mathcal{K}_{\mathcal{S}}^3\right)$. The parameter $\mathcal{K}_s$ operates as a scaling element governing the acquisition of food allergies.

Beyond the confines of allergy acquisition, it is hypothesised that everyone is subject to a uniform mortality rate μ, where the reciprocal μ^{-1} denotes life expectancy. The model also assumes that people taking antacids switch back to the non-sensitized category at a rate δ that corresponds to stopping the medication. Additionally, it is believed that an effective treatment, when available, helps allergic individuals recover, reclassifying them as members of the sensitised group at a rate δ of treatment application. The invariant total population represented by the symbol $N=\mathcal{P}+\mathcal{U}+\mathcal{S}+\mathcal{A}$ is comprised of the population divisions mentioned above. With the introduction of new parameters $k_p=\mathcal{K}_{/}N, k_u=\mathcal{K}_{\mathcal{U}}/N$, and $k_s=\mathcal{K}_{\mathcal{S}}/N$, proportions are defined as $p=\mathcal{P}/N, u=\mathcal{U}/N, s=\mathcal{S}/N$, and $a=\mathcal{A}/N$ in an effort to normalise the analysis. While $\mathcal{K}_{\mathcal{P}}$ deviates from this interpretation because of its linear relationship, the per-capita scaling parameters k_α and k_s assume significance as critical values. A critical threshold uc that separates situations where sensitisation is significantly more pronounced for $u>u^c$ and remains minimal for $u<u^c$ is shown to exist. As a result, the scale of the critical uc directly depends on the size of the scaling parameter $\mathcal{K}_{\mathcal{U}}$. The scaling parameter $\mathcal{K}_S$ governing allergy acquisition follows a similar line of thought. Researchers in [23] introduced the following deterministic model to describe the dynamics of food allergy acquisition by drawing on the accepted definitions of variables and model parameters:

$$\left.\begin{aligned}
\frac{\mathrm{d}\mathcal{P}}{\mathrm{d}t} &= \mu-\mu\mathcal{P}+\delta\mathcal{U}-\alpha\mathcal{P}\frac{\mathcal{U}}{\mathcal{K}_{+}\mathcal{U}}\\
\frac{\mathrm{d}\mathcal{U}}{\mathrm{d}t} &= \alpha\mathcal{P}\frac{\mathcal{U}}{\mathcal{K}_{+}\mathcal{U}}-(\mu+\delta)\mathcal{U}-\beta\frac{\mathcal{U}^2}{\mathcal{K}_{\mathcal{U}}^2+\mathcal{U}^2}\\
\frac{\mathrm{d}\mathcal{S}}{\mathrm{d}t} &= \beta\frac{\mathcal{U}^2}{\mathcal{K}_{\mathcal{U}}^2+\mathcal{U}^2}-\mu s+\varepsilon\mathcal{A}-\gamma\frac{\mathcal{S}^3}{K_{\mathcal{S}}^3+\mathcal{S}^3}\\
\frac{\mathrm{d}\mathcal{A}}{\mathrm{d}t} &= \gamma\frac{\mathcal{S}^3}{\mathcal{K}_{\mathcal{S}}^3+\mathcal{S}^3}-(\mu+\varepsilon)\mathcal{A},\\
\mathcal{P}(0)=\mathcal{P}_0=1-\mathcal{U}_0, &\mathcal{U}(0)=\mathcal{U}_0, \mathcal{S}(0)=\mathcal{S}_0, \mathcal{A}(0)=\mathcal{A}_0.
\end{aligned}\right\} \tag{2.1}$$

Table 1: Summary of the variables and parameters used in model (2.1)

Parameter	Description	Value/day	Reference
μ	Natural mortality rate	3.91389×10^{-5}	[23]
δ	Abandonment rate of antiacid usage	2.0×10^{-4}	[23]
α	Rate of naive persons to become antiacid users	$15.0 \times \alpha^{th}$	[23]
β	Sensitization rate	1.0×10^{-8}	[23]
K_P	Recruitment of antiacid users scaling Factor	1.0×10^{-1}	[23]
K_U	Sensitization scaling factor	1.0×10^{-4}	[23]
γ	Food allergy acquisition rate	2.0×10^{1}	[23]
ε	Recovery rate	1.0×10^{-8}	[23]
K_S	Food allergy acquisition scaling factor	2.1	[23]
P	Fraction of naive population	10^6	[23]
S	Fraction of antiacid users	10^5	[23]
A	Fraction of sensitized persons	10^4	[23]
U	Fraction of food allergic persons	10^{-4}	[23]

A powerful tool for describing memory and hereditary properties inherent to different materials and processes has emerged: fractional derivatives. These effects, which are frequently ignored in models built on traditional integer-order derivatives, represent a key benefit of fractional derivatives. Their importance extends to clarifying the dynamics connecting dissimilar points in a variety of domains, as shown by [27–32]. Although the idea of fractional derivatives and integrals might be seen as a generalisation of their traditional counterparts, it is still a difficult and conceptually complex topic. Fractional derivatives lack the immediate geometrical interpretations that are present in conventional differential operators, such as function trends and convexity, which are frequently connected to fundamental geometric concepts. As a result, this mathematical tool may appear to be somewhat impersonal. The application of fractional calculus is required for the clarification of many physical phenomena, though, as they naturally display a fractional order characteriszation [1]. Fractional derivatives have been given a number of different definitions. Notably, in the references [28, 29], Riemann and Liouville introduced fractional order differentiation using power-law functions. Caputo and Fabrizio offered an alternative strategy in [4], where they introduced a derivative with fractional order rooted in exponential-law functions. The generalised Mittag-Leffler function is used as a non-local, non-singular kernel with strong memory properties in [5] by Atangana and Baleanu to introduce yet another variation of fractional-order derivative. The Food Allergy model (2.1) is reevaluated in the following section of this paper by incorporating a novel operator known as the Caputo-Fabrizio operator. The model,

enhanced by this new operator, assumes the ensuing form:

$$\begin{cases} {}_{a}^{CF}\mathbb{D}_{t}^{\Psi}\mathcal{P} = \mu - \mu\mathcal{P} + \delta\mathcal{U} - \alpha\mathcal{P}\dfrac{\mathcal{U}}{\mathcal{K}_{\mathcal{P}}+\mathcal{U}}, \\ {}_{a}^{CF}\mathbb{D}_{t}^{\Psi}\mathcal{U} = \alpha\mathcal{P}\dfrac{\mathcal{U}}{\mathcal{K}_{\mathcal{P}}+\mathcal{U}} - (\mu+\delta)\mathcal{U} - \beta\dfrac{\mathcal{U}^2}{\mathcal{K}_{\mathcal{U}}^2+\mathcal{U}^2}, \\ {}_{a}^{CF}\mathbb{D}_{t}^{\Psi}\mathcal{S} = \beta\dfrac{\mathcal{U}^2}{\mathcal{K}_{\mathcal{U}}^2+\mathcal{U}^2} - \mu\mathcal{S} + \varepsilon\mathcal{A} - \gamma\dfrac{\mathcal{S}^3}{\mathcal{K}_{\mathcal{S}}^3+\mathcal{S}^3}, \\ {}_{a}^{CF}\mathbb{D}_{t}^{\Psi}\mathcal{A} = \gamma\dfrac{\mathcal{S}^3}{\mathcal{K}_{\mathcal{S}}^3+\mathcal{S}^3} - (\mu+\varepsilon)\mathcal{A}. \\ \mathcal{P}(0) = \mathcal{P}_0, \mathcal{U}(0) = \mathcal{U}_0, \mathcal{S}(0) = \mathcal{S}_0, \mathcal{A}(0) = \mathcal{A}_0. \end{cases} \tag{2.2}$$

3 Preliminaries

Definition 3.1. *The Caputo operator, which is typically used in fractional calculus, is described by the following equation called is integral equation [33]. Let* $\mathbb{F} \in H^1(a,b)$ *and* $b > a$.

$${}_{a}^{C}\mathcal{D}_{t}^{\Psi}\mathbb{F}(t) = \frac{1}{\Gamma(n-\Psi)}\int_{a}^{t}\mathbb{F}^{(n)}(\varsigma)(t-\varsigma)^{n-\Psi-1}d\varsigma, \quad n-1 < \Psi < n \in \mathbb{N} \tag{3.1}$$

$\Gamma(.)$ *represents a gamma function.*

Definition 3.2. *The integral equation in form Caputo operator is given as follow:*

$${}_{a}^{C}\mathcal{J}_{t}^{\Psi}[\mathbb{F}(t)] = \frac{1}{\Gamma(\Psi)}\int_{a}^{t}\mathbb{F}(\varsigma)(t-\varsigma)^{\Psi-1}d\varsigma. \tag{3.2}$$

Definition 3.3. *If we assume that* $\mathbb{F}(t) \in H^1(a,b)$ *and* $b > a$, *A new fractional operator with non-singular kernel was defined by Caputo and Fabrizio in 2015 as follows [34]*

$${}_{a}^{CF}\mathcal{D}_{t}^{\Psi}\mathbb{F}(t) = \frac{\mathbb{M}(\Psi)}{(1-\Psi)}\int_{a}^{t}\frac{d\mathbb{F}(\varsigma)}{d\varsigma}\exp^{-\frac{\Psi(t-\varsigma)}{1-\Psi}} \tag{3.3}$$

Where $\mathbb{M}(0) = \mathbb{M}(1) = 1$ *and thus is a function called normalization function. Furthermore, if* $\mathbb{F} \in H^1(a,b)$

$${}_{a}^{CF}\mathcal{D}_{t}^{\Psi}\mathbb{F}(t) = \frac{\mathbb{M}(\Psi)}{(1-\Psi)}\int_{a}^{t}(\mathbb{F}(t)-\mathbb{F}(\varsigma))\exp^{-\frac{\Psi(t-\varsigma)}{1-\Psi}}. \tag{3.4}$$

Remark 3.4. *If* $x(t) = \frac{(1-\Psi)}{\Psi} \in (0,\infty), \Psi = \frac{1}{(1+x)} \in [0,1]$ *then the equation write above have the following form*

$${}_{a}^{CF}\mathcal{D}_{t}^{\Psi}\mathbb{F}(t) = \frac{\mathbb{M}(x)}{x}\int_{a}^{t}\frac{d\mathbb{F}(\varsigma)}{d\varsigma}\exp\left(-\frac{(t-\varsigma)}{x}\right)d\varsigma, \quad \mathbb{M}(0) = \mathbb{M}(\infty) = 1 \tag{3.5}$$

Further over

$$lim_{x\to 0} \quad \frac{1}{x}\exp\left(-\frac{(t-\varsigma)}{x}\right) = \Delta(t-\Psi), \tag{3.6}$$

Definition 3.5. *Consider the fractional order* Ψ *and* Ψ *ranges in (0,1) , then the fractional integral is defined as*

$${}_{a}^{CF}\mathcal{J}_{t}^{\Psi}\mathbb{F}(t) = \frac{2(1-\Psi)}{(2-\Psi)\mathbb{M}(\Psi)}\mathbb{F}(t) + \frac{2\Psi}{(2-\Psi)\mathbb{M}(\Psi)}\int_{a}^{t}F(\varsigma)d\varsigma. \tag{3.7}$$

Definition 3.6. *Let* $f \in H^1(a,b), a < b, \Psi \in (0,1]$. *The AB derivative of the Caputo type is thus defined as*

$${}_{a}^{ABC}\mathcal{D}_{t}^{\Psi}\mathbb{F} = \frac{B(\Psi)}{(1-\Psi)}\int_{a}^{t}\frac{d\mathbb{F}'(\varsigma)}{d\varsigma}E_{(}\Psi)\left(-\frac{\Psi(t-\varsigma)^{\Psi}}{1-\Psi}\right)d\varsigma. \tag{3.8}$$

Definition 3.7. *The AB fractional integral is given as follows [35]*

$${}_{a}^{ABC}\mathcal{S}_{t}^{\Psi}\mathbb{F}(t) = \frac{(1-\Psi)}{B(\Psi)}\mathbb{F}(t) + \frac{\Psi}{B(\Psi)\Gamma(\Psi)}\int_{a}^{t}\mathbb{F}(x)(t-\varsigma)^{(\Psi-1)}d\varsigma. \tag{3.9}$$

4 Fractional Stability

A fractional extension of the idea of stability is introduced, applicable to systems with non-integer orders, using the idea of fractional variational derivatives. The characteristics of dynamical systems under fractional perturbations can be described using these fractional variational derivatives. We create a framework to evaluate the stability of motion changes that correspond to fractional changes in system variables by using these derivatives. It is important to note that when taken into account in the context of fractional variations, dynamical systems that exhibit instability in the traditional Lyapunov sense may actually display stability.

4.1 Existence of solutions

In this section, we demonstrate the existence of solution for given model by means of fixed point theory. The following is established in [34] on (2.1) using the CF fractional operator:

$$\begin{aligned}
\mathcal{P}(t)-\mathcal{P}(0) &= {}^{CF}_{a}\mathbb{I}^{\Psi}_{t}\left\{\mu-\mu\mathcal{P}+\delta\mathcal{U}-\alpha\mathcal{P}\frac{\mathcal{U}}{\mathcal{K}_{\mathcal{P}}+\mathcal{U}}\right\},\\
\mathcal{U}(t)-\mathcal{U}(0) &= {}^{CF}_{a}\mathbb{I}^{\Psi}_{t}\left\{\alpha\mathcal{P}\frac{\mathcal{U}}{\mathcal{K}_{\mathcal{P}}+\mathcal{U}}-(\mu+\delta)\mathcal{U}-\beta\frac{\mathcal{U}^2}{\mathcal{K}^2_{\mathcal{U}}+\mathcal{U}^2}\right\},\\
\mathcal{S}(t)-\mathcal{S}(0) &= {}^{CF}_{a}\mathbb{I}^{\Psi}_{t}\left\{\beta\frac{\mathcal{U}^2}{\mathcal{K}^2_{\mathcal{U}}+\mathcal{U}^2}-\mu\mathcal{S}+\varepsilon\mathcal{A}-\gamma\frac{\mathcal{S}^3}{\mathcal{K}^3_{\mathcal{S}}+\mathcal{S}^3}\right\},\\
\mathcal{A}(t)-\mathcal{A}(0) &= {}^{CF}_{a}\mathbb{I}^{\Psi}_{t}\left\{\gamma\frac{\mathcal{S}^3}{\mathcal{K}^3_{\mathcal{S}}+\mathcal{S}^3}-(\mu+\varepsilon)\mathcal{A}\right\}.
\end{aligned} \tag{4.1}$$

$$\begin{aligned}
\mathcal{P}(t)-\mathcal{P}(0) =\ & \mathfrak{F}(\Psi)\left\{\mu-\mu\mathcal{P}+\delta\mathcal{U}-\alpha\mathcal{P}\frac{\mathcal{U}}{\mathcal{K}_{\mathcal{P}}+\mathcal{U}}\right\}\\
&-\Delta(\Psi)\int_0^t\left\{\mu-\mu\mathcal{P}+\delta\mathcal{U}-\alpha\mathcal{P}\frac{\mathcal{U}}{\mathcal{K}_{\mathcal{P}}+\mathcal{U}}\right\}ds,\\
\mathcal{U}(t)-\mathcal{U}(0) =\ & \mathfrak{F}(\Psi)\left\{\alpha\mathcal{P}\frac{\mathcal{U}}{\mathcal{K}_{\mathcal{P}}+\mathcal{U}}-(\mu+\delta)\mathcal{U}-\beta\frac{\mathcal{U}^2}{\mathcal{K}^2_{\mathcal{U}}+\mathcal{U}^2}\right\}\\
&-\Delta(\Psi)\int_0^t\left\{\alpha\mathcal{P}\frac{\mathcal{U}}{\mathcal{K}_{\mathcal{P}}+\mathcal{U}}-(\mu+\delta)\mathcal{U}-\beta\frac{\mathcal{U}^2}{\mathcal{K}^2_{\mathcal{U}}+\mathcal{U}^2}\right\}ds,\\
\mathcal{S}(t)-\mathcal{S}(0) =\ & \mathfrak{F}(\Psi)\left\{\beta\frac{\mathcal{U}^2}{\mathcal{K}^2_{\mathcal{U}}+\mathcal{U}^2}-\mu\mathcal{S}+\varepsilon\mathcal{A}-\gamma\frac{\mathcal{S}^3}{\mathcal{K}^3_{\mathcal{S}}+\mathcal{S}^3}\right\}\\
&-\Delta(\Psi)\int_0^t\left\{\beta\frac{\mathcal{U}^2}{\mathcal{K}^2_{\mathcal{U}}+\mathcal{U}^2}-\mu\mathcal{S}+\varepsilon\mathcal{A}-\gamma\frac{\mathcal{S}^3}{\mathcal{K}^3_{\mathcal{S}}+\mathcal{S}^3}\right\}ds,\\
\mathcal{A}(t)-\mathcal{A}(0) =\ & \mathfrak{F}(\Psi)\left\{\gamma\frac{\mathcal{S}^3}{\mathcal{K}^3_{\mathcal{S}}+\mathcal{S}^3}-(\mu+\varepsilon)\mathcal{A}\right\}-\Delta(\Psi)\int_0^t\left\{\gamma\frac{\mathcal{S}^3}{\mathcal{K}^3_{\mathcal{S}}+\mathcal{S}^3}-(\mu+\varepsilon)\mathcal{A}\right\}ds.
\end{aligned} \tag{4.2}$$

Where $\mathfrak{F}(\Psi) = \frac{2(1-\Psi)}{(2-\Psi)\mathbb{M}(\Psi)}$ and $\Delta(\Psi) = \frac{2\Psi}{(2-\Psi)\mathbb{M}(\Psi)}$, Now for simplicity, we replace as follows:

$$\begin{aligned}
\mathcal{J}_1(t,\mathcal{P}) &= \left\{\mu - \mu\mathcal{P} + \delta\mathcal{U} - \alpha\mathcal{P}\frac{\mathcal{U}}{\mathcal{K}_{\mathcal{P}}+\mathcal{U}}\right\},\\
\mathcal{J}_2(t,\mathcal{U}_1) &= \left\{\alpha\mathcal{P}\frac{\mathcal{U}}{\mathcal{K}_{\mathcal{P}}+\mathcal{U}} - (\mu+\delta)\mathcal{U} - \beta\frac{\mathcal{U}^2}{\mathcal{K}_{\mathcal{U}}^2+\mathcal{U}^2}\right\},\\
\mathcal{J}_3(t,\mathcal{S}_2) &= \left\{\beta\frac{\mathcal{U}^2}{\mathcal{K}_{\mathcal{U}}^2+\mathcal{U}^2} - \mu\mathcal{S} + \varepsilon\mathcal{A} - \gamma\frac{\mathcal{S}^3}{\mathcal{K}_{\mathcal{S}}^3+\mathcal{S}^3}\right\},\\
\mathcal{J}_4(t,\mathcal{A}) &= \left\{\beta(\gamma\frac{\mathcal{S}^3}{\mathcal{K}_{\mathcal{S}}^3+\mathcal{S}^3} - (\mu+\varepsilon)\mathcal{A}\right\}.
\end{aligned} \tag{4.3}$$

Theorem 4.1. *The contraction and Lipschitz condition are satisfied by the kernels $\mathcal{J}_1$, $\mathcal{J}_2$, $\mathcal{J}_3$, and $\mathcal{J}_4$, if the inequality shown below is true:*

$$0 \leq \left(\mu + \alpha\frac{M_1}{\mathcal{K}_{\mathcal{P}_1}+M_1}\right) < 1 \tag{4.4}$$

Proof. We start with $\mathcal{J}_1$: Consider that $\mathcal{S}$ and $\mathcal{S}_1$ are two functions, then we calculate in below,

$$\begin{aligned}
\|\mathcal{J}_1(t,\mathcal{P}) - \mathcal{J}_1(t,\mathcal{P}_1)\| &= \left\| \left(\mu - \mu\mathcal{P} + \delta\mathcal{U} - \alpha\mathcal{P}\frac{\mathcal{U}}{\mathcal{K}_{\mathcal{P}}+\mathcal{U}}\right) - \left(\mu - \mu\mathcal{P}_1 + \delta\mathcal{U} - \alpha\mathcal{P}_1\frac{\mathcal{U}}{\mathcal{K}_{\mathcal{P}_1}+\mathcal{U}}\right)\right\|,\\
&= \left\| \left[-\mu - \alpha\frac{\mathcal{U}}{\mathcal{K}_{\mathcal{P}}+\mathcal{U}}\right](\mathcal{P}-\mathcal{P}_1)\right\|.
\end{aligned} \tag{4.5}$$

By utilizing the triangular inequality on Eq.(4.5), we get the following:

$$\begin{aligned}
\|\mathcal{J}_1(t,\mathcal{P}) - \mathcal{J}_1(t,\mathcal{P}_1)\| &\leq \left\| -\mu - \alpha\frac{\mathcal{U}}{\mathcal{K}_{\mathcal{P}}+\mathcal{U}}\right\|\|\mathcal{P}(t) - \mathcal{P}_1(t)\|,\\
&\leq \left\{\mu + \alpha\frac{\mathcal{U}}{\mathcal{K}_{\mathcal{P}_1}+\mathcal{U}}\right\} \times \|(\mathcal{P}(t) - \mathcal{P}_1(t))\|,\\
&\leq \Pi_1 \times \|(\mathcal{P}(t) - \mathcal{P}_1(t))\|
\end{aligned} \tag{4.6}$$

Taking $\Pi_1 = \left\{\mu + \alpha\frac{M_1}{\mathcal{K}_{\mathcal{P}_1}+M_1}\right\}$, Where $\|\mathcal{U}(t)\| \leq M_1$, represent bounded functions, so, it follows

$$\|\mathcal{J}_1(t,\mathcal{P}) - \mathcal{J}_1(t,\mathcal{P}_1) \leq \Pi_1 \times \|(\mathcal{P}(t) - \mathcal{P}_1(t))\|. \tag{4.7}$$

So $\mathcal{J}_1$ satisfies the Lipschitz condition, and if $0 \leq \left\{\mu + \alpha\frac{M_1}{\mathcal{K}_{\mathcal{P}_1}+M_1}\right\} < 1$, then $\mathcal{J}_1$ is a contraction. Similarly, $\mathcal{J}_2$, $\mathcal{J}_3$, and $\mathcal{J}_4$ satisfy the Lipschitz conditions:

$$\begin{aligned}
&\|\mathcal{J}_2(t,\mathcal{U}) - \mathcal{J}_2(t,\mathcal{U}_1) \leq \Pi_2 \times \|(\mathcal{U}(t) - \mathcal{U}_1(t))\|,\\
&\|\mathcal{J}_3(t,\mathcal{S}) - \mathcal{J}_3(t,\mathcal{S}_1) \leq \Pi_3 \times \|(\mathcal{S}(t) - \mathcal{S}_1(t))\|,\\
&\|\mathcal{J}_4(t,\mathcal{A}) - \mathcal{J}_4(t,\mathcal{A}_1) \leq \Pi_4 \times \|(\mathcal{A}(t) - \mathcal{A}_1(t))\|.
\end{aligned} \tag{4.8}$$

(4.2) can be written as follows: With the help of representative kernels, we can write the Eq.(4.2) as follows:

$$\begin{aligned}
\mathcal{P}(t) - \mathcal{P}(0) &= \mathfrak{F}(\Psi)\mathcal{J}_1(t,\mathcal{P}) - \Delta(\Psi)\int_0^t \mathcal{J}_1(s,\mathcal{P})ds,\\
\mathcal{U}(t) - \mathcal{U}(0) &= \mathfrak{F}(\Psi)\mathcal{J}_2(t,\mathcal{U}) - \Delta(\Psi)\int_0^t \mathcal{J}_2(s,\mathcal{U})ds,\\
\mathcal{S}(t) - \mathcal{S}(0) &= \mathfrak{F}(\Psi)\mathcal{J}_3(t,\mathcal{S}) - \Delta(\Psi)\int_0^t \mathcal{J}_3(s,\mathcal{S})ds,\\
\mathcal{A}(t) - \mathcal{A}(0) &= \mathfrak{F}(\Psi)\mathcal{J}_4(t,\mathcal{A}) - \Delta(\Psi)\int_0^t \mathcal{J}_4(s,\mathcal{A})ds.
\end{aligned} \tag{4.9}$$

The accompanying recursive formula is introduced:

$$\begin{aligned}
\mathcal{P}_n(t) &= \mathfrak{F}(\Psi)\mathcal{J}_1(t,\mathcal{P}_{n-1}) - \Delta(\Psi)\int_0^t \mathcal{J}_1(s,\mathcal{P}_{n-1})ds,\\
\mathcal{U}_n(t) &= \mathfrak{F}(\Psi)\mathcal{J}_2(t,\mathcal{U}_{n-1}) - \Delta(\Psi)\int_0^t \mathcal{J}_2(s,\mathcal{U}_{n-1})ds,\\
\mathcal{S}_n(t) &= \mathfrak{F}(\Psi)\mathcal{J}_3(t,\mathcal{S}_{n-1}) - \Delta(\Psi)\int_0^t \mathcal{J}_3(s,\mathcal{S}_{n-1})ds,\\
\mathcal{A}_n(t) &= \mathfrak{F}(\Psi)\mathcal{J}_4(t,\mathcal{A}_{n-1}) - \Delta(\Psi)\int_0^t \mathcal{J}_4(s,\mathcal{A}_{n-1})ds.
\end{aligned} \tag{4.10}$$

We give the ICs

$$\mathcal{P}_0(t) = \mathcal{P}(0), \mathcal{U}_0(t) = \mathcal{U}(0), \mathcal{S}_0(t) = \mathcal{S}(0), \mathcal{A}_0(t) = \mathcal{A}(0), \tag{4.11}$$

The difference among the successive terms, is given by:

$$\begin{aligned}
\delta_{1n}(t) &= \mathcal{P}_n(t) - \mathcal{P}_{n-1} = \mathfrak{F}(\Psi)(\mathcal{J}_1(t,\mathcal{P}_{n-1}) - \mathcal{J}_1(t,\mathcal{P}_{n-2}))\\
&\quad \Delta(\Psi)\int_0^t (\mathcal{J}_1(t,\mathcal{P}_{n-1}) - \mathcal{J}_1(t,\mathcal{P}_{n-2}))ds,\\
\delta_{2n}(t) &= \mathcal{U}_n(t) - \mathcal{U}_{n-1} = \mathfrak{F}(\Psi)(\mathcal{J}_2(t,\mathcal{U}_{n-1}) - \mathcal{J}_2(t,\mathcal{U}_{n-2}))\\
&\quad \Delta(\Psi)\int_0^t (\mathcal{J}_2(t,\mathcal{U}_{n-1}) - \mathcal{J}_2(t,\mathcal{U}_{n-2}))ds,\\
\delta_{3n}(t) &= \mathcal{S}_n(t) - \mathcal{S}_{n-1} = \mathfrak{F}(\Psi)(\mathcal{J}_3(t,\mathcal{S}_{n-1}) - \mathcal{J}_3(t,\mathcal{S}_{n-2}))\\
&\quad \Delta(\Psi)\int_0^t (\mathcal{J}_3(t,\mathcal{S}_{n-1}) - \mathcal{J}_3(t,\mathcal{S}_{n-2}))ds,\\
\delta_{4n}(t) &= \mathcal{A}_n(t) - \mathcal{A}_{n-1} = \mathfrak{F}(\Psi)(\mathcal{J}_4(t,\mathcal{A}_{n-1}) - \mathcal{J}_4(t,\mathcal{A}_{n-2}))\\
&\quad \Delta(\Psi)\int_0^t (\mathcal{J}_4(t,\mathcal{A}_{n-1}) - \mathcal{J}_4(t,\mathcal{A}_{n-2}))ds,
\end{aligned} \tag{4.12}$$

The following should be noted:

$$\begin{cases}
\mathcal{P}_n(t) = \sum_{j=0}^{n} \delta_{1j}(t),\\
\mathcal{U}_n(t) = \sum_{j=0}^{n} \delta_{2j}(t),\\
\mathcal{S}_n(t) = \sum_{j=0}^{n} \delta_{3j}(t),\\
\mathcal{A}_n(t) = \sum_{j=0}^{n} \delta_{4j}(t).
\end{cases} \tag{4.13}$$

We have

$$\begin{aligned}\|\delta_{1n}(t)\| =&\|\mathcal{P}_n(t)-\mathcal{P}_{n-1}(t)\| = \Big\|\mathfrak{F}(\Psi)(\mathcal{J}_1(t,N_{n-1})-\mathcal{J}_1(t,N_{n-2}))\\ &-\Delta(\Psi)\int_0^t(\mathcal{J}_1(t,N_{n-1})-\mathcal{J}_1(t,N_{n-2}))ds\Big\|\end{aligned} \tag{4.14}$$

By using the triangular inequality, the Eq. (4.14) gives us:

$$\begin{aligned}\|\delta_{1n}(t)\| =&\|\mathcal{P}_n(t)-\mathcal{P}_{n-1}(t)\|,\\ &\leq \mathfrak{F}(\Psi)\Big\|(\mathcal{J}_1(t,\mathcal{P}_{n-1})-\mathcal{J}_1(t,\mathcal{P}_{n-2}))\Big\|-\Delta(\Psi)\Big\|\int_0^t(\mathcal{J}_1(t,\mathcal{P}_{n-1})-\mathcal{J}_1(t,\mathcal{P}_{n-2}))\Big\|ds\end{aligned} \tag{4.15}$$

If Lipschitz condition (4.7) holds, we have

$$\begin{aligned}\|\delta_{1n}(t)\| =&\|\mathcal{P}_n(t)-\mathcal{P}_{n-1}(t)\|,\\ &\leq \mathfrak{F}(\Psi)\Pi_1\Big\|\mathcal{P}_{n-1}-\mathcal{P}_{n-2}\Big\|-\Delta(\Psi)\Pi_1\int_0^t\Big\|\mathcal{P}_{n-1}-\mathcal{P}_{n-2}\Big\|ds\end{aligned} \tag{4.16}$$

Then, We have

$$\|\delta_{1n}(t)\| \leq \mathfrak{F}(\Psi)\Pi_1\Big\|\delta_{1_{n-1}}(t)\Big\|-\Delta(\Psi)\Pi_1\int_0^t\Big\|\delta_{1_{n-1}}(t)\Big\|ds \tag{4.17}$$

Similarly, we can find the rest of results

$$\begin{aligned}\|\delta_{2n}(t)\| &\leq \mathfrak{F}(\Psi)\Pi_2\Big\|\delta_{2_{n-1}}(t)\Big\|-\Delta(\Psi)\Pi_2\int_0^t\Big\|\delta_{2_{n-1}}(t)\Big\|ds,\\ \|\delta_{3n}(t)\| &\leq \mathfrak{F}(\Psi)\Pi_3\Big\|\delta_{3_{n-1}}(t)\Big\|-\Delta(\Psi)\Pi_3\int_0^t\Big\|\delta_{3_{n-1}}(t)\Big\|ds,\\ \|\delta_{4n}(t)\| &\leq \mathfrak{F}(\Psi)\Pi_4\Big\|\delta_{4_{n-1}}(t)\Big\|-\Delta(\Psi)\Pi_4\int_0^t\Big\|\delta_{4_{n-1}}(t)\Big\|ds.\end{aligned} \tag{4.18}$$

Theorem 4.2. *The CF Food Allergy model* (2.2) *has unique solution if there exists* t_0 *such that*

$$\mathfrak{F}(\Psi)\Pi_1+\Delta(\Psi)\Pi_1 t_0 \leq 1. \tag{4.19}$$

Proof. Since every one of the functions $\mathcal{P}$, $\mathcal{U}$, $\mathcal{S}$ and $\mathcal{A}$, are bounded, we have shown that the kernels fulfill the Lipschitz condition, in this way by utilizing the recursive technique, we acquire the following succeeding relation by Equations (4.17) and (4.18):

$$\begin{aligned}\|\delta_{1n}(t)\| &\leq \|\mathcal{P}_n(0)\|[\mathfrak{F}(\Psi)\Pi_1+\Delta(\Psi)\Pi_1 t_0]^n,\\ \|\delta_{2n}(t)\| &\leq \|\mathcal{U}_n(0)\|[\mathfrak{F}(\Psi)\Pi_2+\Delta(\Psi)\Pi_2 t_0]^n,\\ \|\delta_{3n}(t)\| &\leq \|\mathcal{S}_n(0)\|[\mathfrak{F}(\Psi)\Pi_3+\Delta(\Psi)\Pi_3 t_0]^n,\\ \|\delta_{4n}(t)\| &\leq \|\mathcal{A}_n(0)\|[\mathfrak{F}(\Psi)\Pi_4+\Delta(\Psi)\Pi_4 t_0]^n.\end{aligned} \tag{4.20}$$

Since we know that the system exists a solution and it's continuous. Therefore, we exhibiting that the above function gives a solution for the Food Allergy model (2.2). we continue as follows:

$$\begin{aligned}\mathcal{P}(t)-\mathcal{P}(0) &= \mathcal{P}_n(t)-\theta_{1n}(t),\\ \mathcal{U}(t)-\mathcal{U}(0) &= \mathcal{U}_n(t)-\theta_{2n}(t),\\ \mathcal{S}(t)-\mathcal{S}(0) &= \mathcal{S}_n(t)-\theta_{3n}(t),\\ \mathcal{A}(t)-\mathcal{A}(0) &= \mathcal{A}_n(t)-\theta_{4n}(t).\end{aligned} \tag{4.21}$$

Therefore

$$\begin{aligned}\|\theta_{1n}(t)\| =&\|\mathfrak{F}(\mathcal{J}_1(t,\mathcal{P})-\mathcal{J}_1(t,\mathcal{P}_{n-1}))-\Delta(\Psi)\int_0^t(\mathcal{J}_1(t,\mathcal{P})-\mathcal{J}_1(t,\mathcal{P}_{n-1}))ds\|,\\ \leq&\mathfrak{F}\|(\mathcal{J}_1(t,\mathcal{P})-\mathcal{J}_1(t,\mathcal{P}_{n-1}))\|-\Delta(\Psi)\int_0^t\|(\mathcal{J}_1(t,N)-\mathcal{J}_1(t,N_{n-1}))\|ds,\\ \leq&\mathfrak{F}\|\mathcal{P}-\mathcal{P}_{n-1}\|-\Delta(\Psi)\int_0^t\|\mathcal{P}-\mathcal{P}_{n-1}\|t.\end{aligned}\tag{4.22}$$

Recursively, this process gives

$$\|\theta_{1n}(t)\|\leq[\mathfrak{F}(\Psi)+\Delta(\Psi)t]^{n+1}\Pi_1^{n+1}d.\tag{4.23}$$

At t_0 we get

$$\|\theta_{1n}(t)\|\leq[\mathfrak{F}(\Psi)+\Delta(\Psi)t_0]^{n+1}\Pi_1^{n+1}d.\tag{4.24}$$

Taking the limit as $n\to\infty$ we get $\|\theta_{1n}(t)\|\to 0$. Also, we can exhibit that $\|\theta_{2n}(t)\|\to 0$, $\|\theta_{3n}(t)\|\to 0$, and $\|\theta_{4n}(t)\|\to 0$, and the proof is done. ∎

4.2 Uniqueness of solutions

To show the uniqueness of a solution, assume that the Food Allergy model has another solution $\mathcal{P},\mathcal{U}$, $\mathcal{S}$, and $\mathcal{A}$. Then we get

$$\mathcal{P}(t)-\mathcal{P}(0)=\mathfrak{F}(\mathcal{J}_1(t,\mathcal{P})-\mathcal{J}_1(t,\mathcal{P}_1))-\Delta(\Psi)\int_0^t(\mathcal{J}_1(t,\mathcal{P})-\mathcal{J}_1(t,\mathcal{P}_1))ds\tag{4.25}$$

Taking the norm, we have

$$\|\mathcal{P}(t)-\mathcal{P}(0)\|\leq\mathfrak{F}\|(\mathcal{J}_1(t,\mathcal{P})-\mathcal{J}_1(t,\mathcal{P}_1))\|-\Delta(\Psi)\int_0^t\|(\mathcal{J}_1(t,\mathcal{P})-\mathcal{J}_1(t,\mathcal{P}_1))\|ds\tag{4.26}$$

From lipschitz condition (4.27) it follows that

$$\|\mathcal{P}(t)-\mathcal{P}(0)\|\leq\mathfrak{F}\|\mathcal{P}-\mathcal{P}_1\|\Pi_1-\Delta(\Psi)\int_0^t\|\mathcal{P}-\mathcal{P}_1\|\Pi_1tds.\tag{4.27}$$

So, we get

$$\|\mathcal{P}(t)-\mathcal{P}(0)\|(1-\mathfrak{F}(\Psi)\Pi_1+\Delta(\Psi)\Pi_1t)\leq 0.\tag{4.28}$$

Theorem 4.3. *The solution of CF Food Allergy model (2.2) is unique subject to the following condition*

$$(1-\mathfrak{F}(\Psi)\Pi_1+\Delta(\Psi)\Pi_1t)>0.\tag{4.29}$$

Proof. Consider Eq.(9.30) holds, then Eq.(9.29) indicate that

$$\|\mathcal{P}(t)-\mathcal{P}(0)\|(1-\mathfrak{F}(\Psi)\Pi_1+\Delta(\Psi)\Pi_1t)\leq 0.\tag{4.30}$$

Further, we get

$$\|\mathcal{P}(t)-\mathcal{P}(0)\|=0\tag{4.31}$$

Therefore, we find

$$\mathcal{P}(t)=\mathcal{P}_1(t)\tag{4.32}$$

In the same manner, following the above process, we find out

$$\begin{aligned}\mathcal{U}(t)&=\mathcal{U}_1(t),\\ \mathcal{S}(t)&=\mathcal{S}_1(t),\\ \mathcal{A}(t)&=\mathcal{A}_1(t).\end{aligned}\tag{4.33}$$

Hence, the uniqueness of the solution of the non-integer Food Allergy system (2.2) has completed. ∎

5 Numerical Modeling

Numerical modeling is a cornerstone of modern scientific investigation, empowering researchers to unlock the natural world's mysteries and address pressing global challenges. As computational techniques advance, the impact of numerical modeling on our understanding of the universe and our ability to shape a better tomorrow will only continue to expand, making it an indispens-able tool in pursuing knowledge and progress. We could use three-step Adams-Bashforth and Newton's polynomial numerical methods in this section for the given fractional order food allergy model (2.2).

5.1 Three-step Adams-Bashforth method with CF operator

This study's numerical approach makes use of the fractional Adams-Bashforth-Moulton (ABM) technique. In the field of numerical analysis, the ABM approach has a long and distinguished history, with origins in Adams' work from the late 19th century. Its development was furthered by Bashforth and Moulton's contributions in the early 20th century, which resulted in its widespread adoption in a variety of disciplines like fluid dynamics, chemical kinetics, and population dynamics. The ABM method has a number of advantages, such as its simplicity, computational effectiveness, and prowess in handling difficult equations. It is easily implemented using common software packages and works by extrapolating data from earlier time steps. The fractional version of the ABM method used in this study is a relatively recent development resulting from recent advances in fractional calculus. This particular variation of the method is particularly effective at solving problems involving fractional derivatives, a common occurrence in many fields of science and engineering. Here we introduce a solution for the Food Allergy model with Caputo-Fabrizio operator based on the Adams-Bashforth scheme

$$\begin{cases} {}^{CF}_{a}\mathbb{D}^{\Psi}_{t}\mathcal{P} = \mu - \mu\mathcal{P} + \delta\mathcal{U} - \alpha\mathcal{P}\dfrac{\mathcal{U}}{\mathcal{K}_{\mathcal{P}}+\mathcal{U}}, \\ {}^{CF}_{a}\mathbb{D}^{\Psi}_{t}\mathcal{U} = \alpha\mathcal{P}\dfrac{\mathcal{U}}{\mathcal{K}_{\mathcal{P}}+\mathcal{U}} - (\mu+\delta)\mathcal{U} - \beta\dfrac{\mathcal{U}^2}{\mathcal{K}^2_{\mathcal{U}}+\mathcal{U}^2}, \\ {}^{CF}_{a}\mathbb{D}^{\Psi}_{t}\mathcal{S} = \beta\dfrac{\mathcal{U}^2}{\mathcal{K}^2_{\mathcal{U}}+\mathcal{U}^2} - \mu\mathcal{S} + \varepsilon\mathcal{A} - \gamma\dfrac{\mathcal{S}^3}{\mathcal{K}^3_{\mathcal{S}}+\mathcal{S}^3}, \\ {}^{CF}_{a}\mathbb{D}^{\Psi}_{t}\mathcal{A} = \gamma\dfrac{\mathcal{S}^3}{\mathcal{K}^3_{\mathcal{S}}+\mathcal{S}^3} - (\mu+\varepsilon)\mathcal{A}. \end{cases} \tag{5.1}$$

Now we can convert (5.1) into the following consideration

$$\begin{aligned} {}^{CF}_{a}\mathbb{D}^{\Psi}_{t}(\mathcal{P}(t)) &= \mathcal{J}_1(\mathcal{P},\mathcal{U},\mathcal{S},\mathcal{A},t), \\ {}^{CF}_{a}\mathbb{D}^{\Psi}_{t}(\mathcal{U}(t)) &= \mathcal{J}_2(\mathcal{P},\mathcal{U},\mathcal{S},\mathcal{A},t), \\ {}^{CF}_{a}\mathbb{D}^{\Psi}_{t}(\mathcal{S}(t)) &= \mathcal{J}_3(\mathcal{P},\mathcal{U},\mathcal{S},\mathcal{A},t), \\ {}^{CF}_{a}\mathbb{D}^{\Psi}_{t}(\mathcal{A}(t)) &= \mathcal{J}_4(\mathcal{P},\mathcal{U},\mathcal{S},\mathcal{A},t). \end{aligned} \tag{5.2}$$

By utilizing the Caputo-Fabrizio integral, we get the following equation

$$\begin{aligned} \mathcal{P}(t) &= \mathcal{P}(0) + \frac{1-\Psi}{\mathbb{M}(\Psi)}\mathcal{J}_1(\mathcal{P},\mathcal{U},\mathcal{S},\mathcal{A},t) + \frac{\Psi}{\mathbb{M}(\Psi)}\int_0^t \mathcal{J}_1(\mathcal{P},\mathcal{U},\mathcal{S},\mathcal{A},\varsigma)d\varsigma, \\ \mathcal{U}(t) &= \mathcal{U}(0) + \frac{1-\Psi}{\mathbb{M}(\Psi)}\mathcal{J}_2(\mathcal{P},\mathcal{U},\mathcal{S},\mathcal{A},t) + \frac{\Psi}{\mathbb{M}(\Psi)}\int_0^t \mathcal{J}_2(\mathcal{P},\mathcal{U},\mathcal{S},\mathcal{A},\varsigma)d\varsigma, \\ \mathcal{S}(t) &= \mathcal{S}(0) + \frac{1-\Psi}{\mathbb{M}(\Psi)}\mathcal{J}_3(\mathcal{P},\mathcal{U},\mathcal{S},\mathcal{A},t) + \frac{\Psi}{\mathbb{M}(\Psi)}\int_0^t \mathcal{J}_3(\mathcal{P},\mathcal{U},\mathcal{S},\mathcal{A},\varsigma)d\varsigma, \\ \mathcal{A}(t) &= \mathcal{A}(0) + \frac{1-\Psi}{\mathbb{M}(\Psi)}\mathcal{J}_4(\mathcal{P},\mathcal{U},\mathcal{S},\mathcal{A},t) + \frac{\Psi}{\mathbb{M}(\Psi)}\int_0^t \mathcal{J}_4(\mathcal{P},\mathcal{U},\mathcal{S},\mathcal{A},\varsigma)d\varsigma. \end{aligned} \tag{5.3}$$

Where $t = t_{m+1}$:

$$\begin{aligned}
\mathcal{P}(t_{m+1}) &= \mathcal{P}(0) + \frac{1-\Psi}{\mathbb{M}(\Psi)}\mathcal{J}_1(\mathcal{P}^m,\mathcal{U}^m,\mathcal{S}^m,\mathcal{A}^m,t_m) + \frac{\Psi}{\mathbb{M}(\Psi)}\int_0^{t_{m+1}} \mathcal{J}_1(\mathcal{P},\mathcal{U},\mathcal{S},\mathcal{A},\varsigma)d\varsigma,\\
\mathcal{U}(t_{m+1}) &= \mathcal{U}(0) + \frac{1-\Psi}{\mathbb{M}(\Psi)}\mathcal{J}_2(\mathcal{P}^m,\mathcal{U}^m,\mathcal{S}^m,\mathcal{A}^m,t_m) + \frac{\Psi}{\mathbb{M}(\Psi)}\int_0^{t_{m+1}} \mathcal{J}_1(\mathcal{P},\mathcal{U},\mathcal{S},\mathcal{A},\varsigma)d\varsigma,\\
\mathcal{S}(t_{m+1}) &= \mathcal{S}(0) + \frac{1-\Psi}{\mathbb{M}(\Psi)}\mathcal{J}_3(\mathcal{P}^m,\mathcal{U}^m,\mathcal{S}^m,\mathcal{A}^m,t_m) + \frac{\Psi}{\mathbb{M}(\Psi)}\int_0^{t_{m+1}} \mathcal{J}_1(\mathcal{P},\mathcal{U},\mathcal{S},\mathcal{A},\varsigma)d\varsigma,\\
\mathcal{A}(t_{m+1}) &= \mathcal{A}(0) + \frac{1-\Psi}{\mathbb{M}(\Psi)}\mathcal{J}_4(\mathcal{P}^m,\mathcal{U}^m,\mathcal{S}^m,\mathcal{A}^m,t_m) + \frac{\Psi}{\mathbb{M}(\Psi)}\int_0^{t_{m+1}} \mathcal{J}_1(\mathcal{P},\mathcal{U},\mathcal{S},\mathcal{A},\varsigma)d\varsigma.
\end{aligned} \tag{5.4}$$

And at point $t = t_m$:

$$\begin{aligned}
\mathcal{P}(t_m) &= \mathcal{P}(0) + \frac{1-\Psi}{\mathbb{M}(\Psi)}\mathcal{J}_1(\mathcal{P}^{m-1},\mathcal{U}^{m-1},\mathcal{S}^{m-1},\mathcal{A}^{m-1},t_{m-1})\\
&\quad + \frac{\Psi}{\mathbb{M}(\Psi)}\int_0^{t_m} \mathcal{J}_1(\mathcal{P},\mathcal{U},\mathcal{S},\mathcal{A},\varsigma)d\varsigma,\\
\mathcal{U}(t_m) &= \mathcal{U}(0) + \frac{1-\Psi}{\mathbb{M}(\Psi)}\mathcal{J}_2(\mathcal{P}^{m-1},\mathcal{U}^{m-1},\mathcal{S}^{m-1},\mathcal{A}^{m-1},t_{m-1})\\
&\quad + \frac{\Psi}{\mathbb{M}(\Psi)}\int_0^{t_m} \mathcal{J}_2(\mathcal{P},\mathcal{U},\mathcal{S},\mathcal{A},\varsigma)d\varsigma,\\
\mathcal{S}(t_m) &= \mathcal{S}(0) + \frac{1-\Psi}{\mathbb{M}(\Psi)}\mathcal{J}_3(\mathcal{P}^{m-1},\mathcal{U}^{m-1},\mathcal{S}^{m-1},\mathcal{A}^{m-1},t_{m-1})\\
&\quad + \frac{\Psi}{\mathbb{M}(\Psi)}\int_0^{t_m} \mathcal{J}_3(\mathcal{P},\mathcal{U},\mathcal{S},\mathcal{A},\varsigma)d\varsigma,\\
\mathcal{A}(t_m) &= \mathcal{A}(0) + \frac{1-\Psi}{\mathbb{M}(\Psi)}\mathcal{J}_4(\mathcal{P}^{m-1},\mathcal{U}^{m-1},\mathcal{S}^{m-1},\mathcal{A}^{m-1},t_{m-1})\\
&\quad + \frac{\Psi}{\mathbb{M}(\Psi)}\int_0^{t_m} \mathcal{J}_4(\mathcal{P},\mathcal{U},\mathcal{S},\mathcal{A},\varsigma)d\varsigma.
\end{aligned} \tag{5.5}$$

Now we subtract the condition ((5.4) and (5.5)), then we have the following result

$$\begin{aligned}
\mathcal{P}(t_{m+1}) &= \mathcal{P}(t_m) + \frac{1-\Psi}{\mathbb{M}(\Psi)}(\mathcal{J}_1(\mathcal{P}^m,\mathcal{U}^m,\mathcal{S}^m,\mathcal{A}^m,t_m)\\
&\quad - \mathcal{J}_1(\mathcal{P}^{m-1},\mathcal{U}^{m-1},\mathcal{S}^{m-1},\mathcal{A}^{m-1},t_{m-1})) + \frac{\Psi}{\mathbb{M}(\Psi)}\int_{t_m}^{t_{m+1}} \mathcal{J}_1(\mathcal{P},\mathcal{U},\mathcal{S},\mathcal{A},\varsigma)d\varsigma,\\
\mathcal{U}(t_{m+1}) &= \mathcal{U}(t_m) + \frac{1-\Psi}{\mathbb{M}(\Psi)}(\mathcal{J}_2(\mathcal{P}^m,\mathcal{U}^m,\mathcal{S}^m,\mathcal{A}^m,t_m)\\
&\quad - \mathcal{J}_2(\mathcal{P}^{m-1},\mathcal{U}^{m-1},\mathcal{S}^{m-1},\mathcal{A}^{m-1},t_{m-1})) + \frac{\Psi}{\mathbb{M}(\Psi)}\int_{t_m}^{t_{m+1}} \mathcal{J}_2(\mathcal{P},\mathcal{U},\mathcal{S},\mathcal{A},\varsigma)d\varsigma,\\
\mathcal{S}(t_{m+1}) &= \mathcal{S}(t_m) + \frac{1-\Psi}{\mathbb{M}(\Psi)}(\mathcal{J}_3(\mathcal{P}^m,\mathcal{U}^m,\mathcal{S}^m,\mathcal{A}^m,t_m)\\
&\quad - \mathcal{J}_3(\mathcal{P}^{m-1},\mathcal{U}^{m-1},\mathcal{S}^{m-1},\mathcal{A}^{m-1},t_{m-1})) + \frac{\Psi}{\mathbb{M}(\Psi)}\int_{t_m}^{t_{m+1}} \mathcal{J}_3(\mathcal{P},\mathcal{U},\mathcal{S},\mathcal{A},\varsigma)d\varsigma,\\
\mathcal{A}(t_{m+1}) &= \mathcal{A}(t_m) + \frac{1-\Psi}{\mathbb{M}(\Psi)}(\mathcal{J}_4(\mathcal{P}^m,\mathcal{U}^m,\mathcal{S}^m,\mathcal{A}^m,t_m)\\
&\quad - \mathcal{J}_4(\mathcal{P}^{m-1},\mathcal{U}^{m-1},\mathcal{S}^{m-1},\mathcal{A}^{m-1},t_{m-1})) + \frac{\Psi}{\mathbb{M}(\Psi)}\int_{t_m}^{t_{m+1}} \mathcal{J}_4(\mathcal{P},\mathcal{U},\mathcal{S},\mathcal{A},\varsigma)d\varsigma.
\end{aligned} \tag{5.6}$$

Where

$$\int_{t_m}^{t_{m+1}} \mathcal{J}_1(\mathcal{P},\mathcal{U},\mathcal{S},\mathcal{A},\varsigma)d\varsigma = \int_{t_m}^{t_{m+1}} \left[\frac{\mathcal{J}_1(\mathcal{P}_m,\mathcal{U}_m,\mathcal{S}_m,\mathcal{A}_m,\varsigma_m)}{h}(t-t_m)\right.$$
$$\left. - \frac{\mathcal{J}_1(\mathcal{P}_{m-1},\mathcal{U}_{m-1},\mathcal{S}_{m-1},\mathcal{A}_{m-1},\varsigma_{m-1})}{h}(t-t_{m-1}) + \frac{\mathcal{J}_1(\mathcal{P}_{m-2},\mathcal{U}_{m-2},\mathcal{S}_{m-2},\mathcal{A}_{m-2},\varsigma_{m-2})}{h}(t-t_{m-2})\right],$$
$$\int_{t_m}^{t_{m+1}} \mathcal{J}_2(\mathcal{P},\mathcal{U},\mathcal{S},\mathcal{A},\varsigma)d\varsigma = \int_{t_m}^{t_{m+1}} \left[\frac{\mathcal{J}_2(\mathcal{P}_m,\mathcal{U}_m,\mathcal{S}_m,\mathcal{A}_m,\varsigma_m)}{h}(t-t_m)\right.$$
$$\left. - \frac{\mathcal{J}_2(\mathcal{P}_{m-1},\mathcal{U}_{m-1},\mathcal{S}_{m-1},\mathcal{A}_{m-1},\varsigma_{m-1})}{h}(t-t_{m-1}) + \frac{\mathcal{J}_2(\mathcal{P}_{m-2},\mathcal{U}_{m-2},\mathcal{S}_{m-2},\mathcal{A}_{m-2},\varsigma_{m-2})}{h}(t-t_{m-2})\right],$$
$$\int_{t_m}^{t_{m+1}} \mathcal{J}_3(\mathcal{P},\mathcal{U},\mathcal{S},\mathcal{A},\varsigma)d\varsigma = \int_{t_m}^{t_{m+1}} \left[\frac{\mathcal{J}_3(\mathcal{P}_m,\mathcal{U}_m,\mathcal{S}_m,\mathcal{A}_m,\varsigma_m)}{h}(t-t_m)\right.$$
$$\left. - \frac{\mathcal{J}_3(\mathcal{P}_{m-1},\mathcal{U}_{m-1},\mathcal{S}_{m-1},\mathcal{A}_{m-1},\varsigma_{m-1})}{h}(t-t_{m-1}) + \frac{\mathcal{J}_3(\mathcal{P}_{m-2},\mathcal{U}_{m-2},\mathcal{S}_{m-2},\mathcal{A}_{m-2},\varsigma_{m-2})}{h}(t-t_{m-2})\right],$$
$$\int_{t_m}^{t_{m+1}} \mathcal{J}_4(\mathcal{P},\mathcal{U},\mathcal{S},\mathcal{A},\varsigma)d\varsigma = \int_{t_m}^{t_{m+1}} \left[\frac{\mathcal{J}_4(\mathcal{P}_m,\mathcal{U}_m,\mathcal{S}_m,\mathcal{A}_m,\varsigma_m)}{h}(t-t_m)\right.$$
$$\left. - \frac{\mathcal{J}_4(\mathcal{P}_{m-1},\mathcal{U}_{m-1},\mathcal{S}_{m-1},\mathcal{A}_{m-1},\varsigma_{m-1})}{h}(t-t_{m-1}) + \frac{\mathcal{J}_4(\mathcal{P}_{m-2},\mathcal{U}_{m-2},\mathcal{S}_{m-2},\mathcal{A}_{m-2},\varsigma_{m-2})}{h}(t-t_{m-2})\right]. \tag{5.7}$$

$$\int_{t_m}^{t_{m+1}} \mathcal{J}_1(\mathcal{P},\mathcal{U},\mathcal{S},\mathcal{A},\varsigma)d\varsigma = \frac{23h}{12}\mathcal{J}_1(\mathcal{P}_m,\mathcal{U}_m,\mathcal{S}_m,\mathcal{A}_m,\varsigma_m) - \frac{16h}{12}\mathcal{J}_1(\mathcal{P}_{m-1},\mathcal{U}_{m-1},\mathcal{S}_{m-1},\mathcal{A}_{m-1},\varsigma_{m-1})$$
$$+\frac{5h}{12}\mathcal{J}_1(\mathcal{P}_{m-2},\mathcal{U}_{m-2},\mathcal{S}_{m-2},\mathcal{A}_{m-2},\varsigma_{m-2}),$$
$$\int_{t_m}^{t_{m+1}} \mathcal{J}_2(\mathcal{P},\mathcal{U},\mathcal{S},\mathcal{A},\varsigma)d\varsigma = \frac{23h}{12}\mathcal{J}_2(\mathcal{P}_m,\mathcal{U}_m,\mathcal{S}_m,\mathcal{A}_m,\varsigma_m) - \frac{16h}{12}\mathcal{J}_2(\mathcal{P}_{m-1},\mathcal{U}_{m-1},\mathcal{S}_{m-1},\mathcal{A}_{m-1},\varsigma_{m-1})$$
$$+\frac{5h}{12}\mathcal{J}_2(\mathcal{P}_{m-2},\mathcal{U}_{m-2},\mathcal{S}_{m-2},\mathcal{A}_{m-2},\varsigma_{m-2}),$$
$$\int_{t_m}^{t_{m+1}} \mathcal{J}_3(\mathcal{P},\mathcal{U},\mathcal{S},\mathcal{A},\varsigma)d\varsigma = \frac{23h}{12}\mathcal{J}_3(\mathcal{P}_m,\mathcal{U}_m,\mathcal{S}_m,\mathcal{A}_m,\varsigma_m) - \frac{16h}{12}\mathcal{J}_3(\mathcal{P}_{m-1},\mathcal{U}_{m-1},\mathcal{S}_{m-1},\mathcal{A}_{m-1},\varsigma_{m-1})$$
$$+\frac{5h}{12}\mathcal{J}_3(\mathcal{P}_{m-2},\mathcal{U}_{m-2},\mathcal{S}_{m-2},\mathcal{A}_{m-2},\varsigma_{m-2}),$$
$$\int_{t_m}^{t_{m+1}} \mathcal{J}_4(\mathcal{P},\mathcal{U},\mathcal{S},\mathcal{A},\varsigma)d\varsigma = \frac{23h}{12}\mathcal{J}_4(\mathcal{P}_m,\mathcal{U}_m,\mathcal{S}_m,\mathcal{A}_m,\varsigma_m) - \frac{16h}{12}\mathcal{J}_4(\mathcal{P}_{m-1},\mathcal{U}_{m-1},\mathcal{S}_{m-1},\mathcal{A}_{m-1},\varsigma_{m-1})$$
$$+\frac{5h}{12}\mathcal{J}_4(\mathcal{P}_{m-2},\mathcal{U}_{m-2},\mathcal{S}_{m-2},\mathcal{A}_{m-2},\varsigma_{m-2}).$$

Therefore

$$\begin{aligned}
\mathcal{P}(t_{m+1}) =&\mathcal{P}(t_m) + \frac{1-\Psi}{\mathbb{M}(\Psi)}[\mathcal{J}_1(\mathcal{P}_m, \mathcal{U}_m, \mathcal{S}_m, \mathcal{A}_m, t_m) \\
&-\mathcal{J}_1(\mathcal{P}_{m-1}, \mathcal{U}_{m-1}, \mathcal{S}_{m-1}, \mathcal{A}_{m-1}, t_{m-1})] + \frac{\Psi h}{12\mathbb{M}(\Psi)}[23\mathcal{J}_1(\mathcal{P}_m, \mathcal{U}_m, \mathcal{S}_m, \mathcal{A}_m, \varsigma_m) \\
&-16\mathcal{J}_1(\mathcal{P}_{m-1}, \mathcal{U}_{m-1}, \mathcal{S}_{m-1}, \mathcal{A}_{m-1}, \varsigma_{m-1}) + 5\mathcal{J}_1(\mathcal{P}_{m-2}, \mathcal{U}_{m-2}, \mathcal{S}_{m-2}, \mathcal{A}_{m-2}, \varsigma_{m-2})], \\
\mathcal{U}(t_{m+1}) =&\mathcal{U}(t_m) + \frac{1-\Psi}{\mathbb{M}(\Psi)}[\mathcal{J}_2(\mathcal{P}_m, \mathcal{U}_m, \mathcal{S}_m, \mathcal{A}_m, t_m) \\
&-\mathcal{J}_2(\mathcal{P}_{m-1}, \mathcal{U}_{m-1}, \mathcal{S}_{m-1}, \mathcal{A}_{m-1}, t_{m-1})] + \frac{\Psi h}{12\mathbb{M}(\Psi)}[23\mathcal{J}_2(\mathcal{P}_m, \mathcal{U}_m, \mathcal{S}_m, \mathcal{A}_m, \varsigma_m) \\
&-16\mathcal{J}_2(\mathcal{P}_{m-1}, \mathcal{U}_{m-1}, \mathcal{S}_{m-1}, \mathcal{A}_{m-1}, \varsigma_{m-1}) + 5\mathcal{J}_2(\mathcal{P}_{m-2}, \mathcal{U}_{m-2}, \mathcal{S}_{m-2}, \mathcal{A}_{m-2}, \varsigma_{m-2})], \\
\mathcal{S}(t_{m+1}) =&\mathcal{S}(t_m) + \frac{1-\Psi}{\mathbb{M}(\Psi)}[\mathcal{J}_3(\mathcal{P}_m, \mathcal{U}_m, \mathcal{S}_m, \mathcal{A}_m, t_m) \\
&-\mathcal{J}_3(\mathcal{P}_{m-1}, \mathcal{U}_{m-1}, \mathcal{S}_{m-1}, \mathcal{A}_{m-1}, t_{m-1})] + \frac{\Psi h}{12\mathbb{M}(\Psi)}[23\mathcal{J}_3(\mathcal{P}_m, \mathcal{U}_m, \mathcal{S}_m, \mathcal{A}_m, \varsigma_m) \\
&-16\mathcal{J}_3(\mathcal{P}_{m-1}, \mathcal{U}_{m-1}, \mathcal{S}_{m-1}, \mathcal{A}_{m-1}, \varsigma_{m-1}) + 5\mathcal{J}_3(\mathcal{P}_{m-2}, \mathcal{U}_{m-2}, \mathcal{S}_{m-2}, \mathcal{A}_{m-2}, \varsigma_{m-2})], \\
\mathcal{A}(t_{m+1}) =&\mathcal{A}(t_m) + \frac{1-\Psi}{\mathbb{M}(\Psi)}[\mathcal{J}_4(\mathcal{P}_m, \mathcal{U}_m, \mathcal{S}_m, \mathcal{A}_m, t_m) \\
&-\mathcal{J}_4(\mathcal{P}_{m-1}, \mathcal{U}_{m-1}, \mathcal{S}_{m-1}, \mathcal{A}_{m-1}, t_{m-1})] + \frac{\Psi h}{12\mathbb{M}(\Psi)}[23\mathcal{J}_4(\mathcal{P}_m, \mathcal{U}_m, \mathcal{S}_m, \mathcal{A}_m, \varsigma_m) \\
&-16\mathcal{J}_4(\mathcal{P}_{m-1}, \mathcal{U}_{m-1}, \mathcal{S}_{m-1}, \mathcal{A}_{m-1}, \varsigma_{m-1}) + 5\mathcal{J}_4(\mathcal{P}_{m-2}, \mathcal{U}_{m-2}, \mathcal{S}_{m-2}, \mathcal{A}_{m-2}, \varsigma_{m-2})].
\end{aligned} \tag{5.8}$$

Which implies that

(5.9)

5.2 Numerical scheme via Newton's polynomial

Here, we introduce a numerical approach to dealing with fractional-order systems that is essentially based on Newton's polynomial [37]. In their works [38–40], Atangana and Seda pioneered the use of novel COVID-19 models and used Newton's polynomial as a numerical tool for their solutions. It is important to recognise the fundamental importance of Newton's interpolation in numerical methods, particularly in the context of image processing. This strategy is a time-tested, conventional approach that has been widely used for interpolation. The provided dataset has been specifically tailored to the interpolation functions used in the majority of conventional methodologies. In this study, we concentrate on Newton's polynomial interpolation because it has many advantages over other methods. It should be noted that this method of interpolation demonstrates superior convergence properties, ease of implementation, mathematical robustness, and versatility across various dimensions like differentiation and integration. These polynomials' non-integer order derivatives can also be easily calculated. Additionally, by appropriately adjusting the parameter value, the value of the Newton-type interpolation function can be quickly changed within the region of interest. The structure and arrangement of the interpolating surfaces and curves can be easily changed depending on the inherent properties and

geometric requirements. In light of these factors, we will proceed to restate the model as follows:

$$\begin{cases} {}^{CF}_{a}\mathbb{D}^{\Psi}_{t}\mathcal{P} = \mu - \mu\mathcal{P} + \delta\mathcal{U} - \alpha\mathcal{P}\dfrac{\mathcal{U}}{\mathcal{K}_{\mathcal{P}}+\mathcal{U}}, \\ {}^{CF}_{a}\mathbb{D}^{\Psi}_{t}\mathcal{U} = \alpha\mathcal{P}\dfrac{\mathcal{U}}{\mathcal{K}_{\mathcal{P}}+\mathcal{U}} - (\mu+\delta)\mathcal{U} - \beta\dfrac{\mathcal{U}^2}{\mathcal{K}^2_{\mathcal{U}}+\mathcal{U}^2}, \\ {}^{CF}_{a}\mathbb{D}^{\Psi}_{t}\mathcal{S} = \beta\dfrac{\mathcal{U}^2}{\mathcal{K}^2_{\mathcal{U}}+\mathcal{U}^2} - \mu\mathcal{S} + \varepsilon\mathcal{A} - \gamma\dfrac{\mathcal{S}^3}{\mathcal{K}^3_{\mathcal{S}}+\mathcal{S}^3}, \\ {}^{CF}_{a}\mathbb{D}^{\Psi}_{t}\mathcal{A} = \gamma\dfrac{\mathcal{S}^3}{\mathcal{K}^3_{\mathcal{S}}+\mathcal{S}^3} - (\mu+\varepsilon)\mathcal{A}. \\ \mathcal{P}(0) = \mathcal{P}_0, \mathcal{U}(0) = \mathcal{U}_0, \mathcal{S}(0) = \mathcal{S}_0, \mathcal{A}(0) = \mathcal{A}_0. \end{cases} \tag{5.10}$$

For simplicity, we write the above equation as follows;

$$\begin{cases} {}^{\mathrm{CF}}_{0}\mathcal{D}^{\Psi}_{t}\mathcal{P} &= \mathcal{P}^*(t,\mathcal{P},\mathcal{U},\mathcal{S},\mathcal{A}), \\ {}^{\mathrm{CF}}_{0}\mathcal{D}^{\Psi}_{t}\mathcal{U} &= \mathcal{U}^*(t,\mathcal{P},\mathcal{U},\mathcal{S},\mathcal{A}), \\ {}^{\mathrm{CF}}_{0}\mathcal{D}^{\Psi}_{t}\mathcal{S} &= \mathcal{S}^*(t,\mathcal{P},\mathcal{U},\mathcal{S},\mathcal{A}), \\ {}^{\mathrm{CF}}_{0}\mathcal{D}^{\Psi}_{t}\mathcal{A} &= \mathcal{A}^*(t,\mathcal{P},\mathcal{U},\mathcal{S},\mathcal{A}). \end{cases} \tag{5.11}$$

After applying fractional integral with exponential kernel and putting Newton polynomial into these equations, we can solve our model as follows;

$$\begin{aligned} \mathcal{P}^{v+1} &= \mathcal{P}^v + \frac{1-\Psi}{M(\Psi)}\begin{bmatrix} \mathcal{P}^*(t_v,\mathcal{P}^v,\mathcal{U}^v,\mathcal{S}^v,\mathcal{A}^v) \\ -\mathcal{P}^*(t_{v-1},\mathcal{P}^{v-1},\mathcal{U}^{v-1},\mathcal{S}^v,\mathcal{A}^{v-1}) \end{bmatrix} \\ &\quad + \frac{\Psi}{M(\Psi)}\begin{Bmatrix} \frac{23}{12}\mathcal{P}^*(t_v,\mathcal{P}^v,\mathcal{U}^v,\mathcal{S}^v,\mathcal{A}^v,)\Delta t \\ -\frac{4}{3}\mathcal{P}^*(t_{v-1},\mathcal{P}^{v-1},\mathcal{U}^{v-1},\mathcal{S}^v,\mathcal{A}^{v-1})\Delta t \\ +\frac{5}{12}\mathcal{P}^*(t_{v-2},\mathcal{P}^{v-2},\mathcal{U}^{v-2},\mathcal{S}^{v-2},\mathcal{A}^{v-2})\Delta t \end{Bmatrix} \end{aligned}$$

$$\begin{aligned} \mathcal{U}^{v+1} &= \mathcal{U}^v + \frac{1-\Psi}{M(\Psi)}\begin{bmatrix} \mathcal{U}^*(t_v,\mathcal{P}^v,\mathcal{U}^v,\mathcal{S}^v,\mathcal{A}^v,) \\ -\mathcal{U}^*(t_{v-1},\mathcal{P}^{v-1},\mathcal{U}^{v-1},\mathcal{S}^v,\mathcal{A}^{v-1}) \end{bmatrix} \\ &\quad + \frac{\Psi}{M(\Psi)}\begin{Bmatrix} \frac{23}{12}\mathcal{U}^*(t_v,\mathcal{P}^v,\mathcal{U}^v,\mathcal{S}^v,\mathcal{A}^v,)\Delta t \\ -\frac{4}{3}\mathcal{U}^*(t_{v-1},\mathcal{P}^{v-1},\mathcal{U}^{v-1},\mathcal{S}^v,\mathcal{A}^{v-1})\Delta t \\ +\frac{5}{12}\mathcal{U}^*(t_{v-2},\mathcal{P}^{v-2},\mathcal{U}^{v-2},\mathcal{S}^{v-2},\mathcal{A}^{v-2})\Delta t \end{Bmatrix} \end{aligned}$$

$$\begin{aligned} \mathcal{S}^{v+1} &= \mathcal{S}^v + \frac{1-\Psi}{M(\Psi)}\begin{bmatrix} \mathcal{S}^*(t_v,\mathcal{S}^v,\mathcal{U}^v,\mathcal{S}^v,\mathcal{A}^v,) \\ -\mathcal{S}^*(t_{v-1},\mathcal{P}^{v-1},\mathcal{U}^{v-1},\mathcal{S}^v,\mathcal{A}^{v-1}) \end{bmatrix} \\ &\quad + \frac{\Psi}{M(\Psi)}\begin{Bmatrix} \frac{23}{12}\mathcal{S}^*(t_v,\mathcal{P}^v,\mathcal{U}^v,\mathcal{S}^v,\mathcal{A}^v,)\Delta t \\ -\frac{4}{3}\mathcal{S}^*(t_{v-1},\mathcal{P}^{v-1},\mathcal{U}^{v-1},\mathcal{S}^v,\mathcal{A}^{v-1})\Delta t \\ +\frac{5}{12}\mathcal{S}^*(t_{v-2},\mathcal{P}^{v-2},\mathcal{U}^{v-2},\mathcal{S}^{v-2},\mathcal{A}^{v-2})\Delta t \end{Bmatrix} \end{aligned}$$

$$\begin{aligned} \mathcal{A}^{v+1} &= \mathcal{A}^v + \frac{1-\Psi}{M(\Psi)}\begin{bmatrix} \mathcal{A}^*(t_v,\mathcal{S}^v,\mathcal{U}^v,\mathcal{S}^v,\mathcal{A}^v,) \\ -\mathcal{A}^*(t_{v-1},\mathcal{P}^{v-1},\mathcal{U}^{v-1},\mathcal{S}^v,\mathcal{A}^{v-1}) \end{bmatrix} \\ &\quad + \frac{\Psi}{M(\Psi)}\begin{Bmatrix} \frac{23}{12}\mathcal{A}^*(t_v,\mathcal{P}^v,\mathcal{U}^v,\mathcal{S}^v,\mathcal{A}^v,)\Delta t \\ -\frac{4}{3}\mathcal{A}^*(t_{v-1},\mathcal{P}^{v-1},\mathcal{U}^{v-1},\mathcal{S}^v,\mathcal{A}^{v-1})\Delta t \\ +\frac{5}{12}\mathcal{A}^*(t_{v-2},\mathcal{P}^{v-2},\mathcal{U}^{v-2},\mathcal{S}^{v-2},\mathcal{A}^{v-2})\Delta t \end{Bmatrix} \end{aligned}$$

5.3 Graphical Results

We simulate the Caputo-Fabrizio (CF) fractional-order model (2.2) in this section of the manuscript using the previously discussed three-step Adams-Bashforth (ABM) and Newton's polynomial numerical techniques. These simulations' goals are to learn more about the model's dynamics and investigate the implications of changing the fractional order parameter Ψ. The simulation results are tabulated in Table 1 and then plotted to show how various state variables behave under various Ψ values. Utilising MATLAB 2019, the simulation process has a time range of 0 to 5 steps. We thoroughly investigate how various fractional order values affect the dynamics of the model through the executed numerical simulations. In particular, for fractional order values ranging from 0.50 to 1, we examine the behaviour of each class within the system (2.2). The ensuing Figures 1(a) to 1(d) in the following section depict these dynamics. The population of naive people decreases as the fractional order Ψ decreases, as shown in Figure 1(a), indicating a decreasing influence of naive people on the system as the order becomes more fractional. We can see the increase in antiacid usage over time in Figure 1(b), though it eventually reaches an equilibrium state after a certain amount of time. Figure 1(c) also shows a declining trend over time with declining Ψ values in the population of sensitised people. Similar to Figure 1(c), Figure 1(d) shows the population of people with food allergies and how they change over time. The simulation results show how responsive the system is to changing non-integer order parameters Ψ. Figure 2 also shows the long-term simulation results of the ABM method. Additionally, as shown in Figures 3 and 4, we compare these results with simulations performed using the Newton Polynomial approach, revealing similar trends between the two numerical approaches. Figures 5 and 6 show the effects of scaling factors K_P and K_S on each state variable under a fixed fractional order $\Psi = 1$, respectively. This investigation is done to better understand how the system behaves. These visualisations offer insightful information about how the system reacts to changes in the acquisition scaling factors for food allergies and the recruitment of antiacid users. In conclusion, the simulation results obtained using the Newton Polynomial and ABM methods provide in-depth understanding of the dynamics of the proposed CF fractional-order model. The exploration of various fractional order parameters and the effects of scaling factors provide insight into how the food allergy system behaves under various circumstances. These discoveries help us better understand the underlying dynamics and facilitate the creation of sensible management strategies.

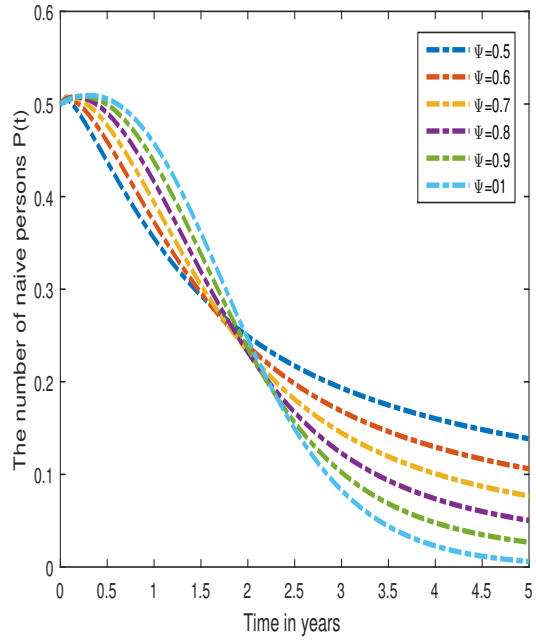

((a)) The number of naive persons $\mathcal{P}(t)$.

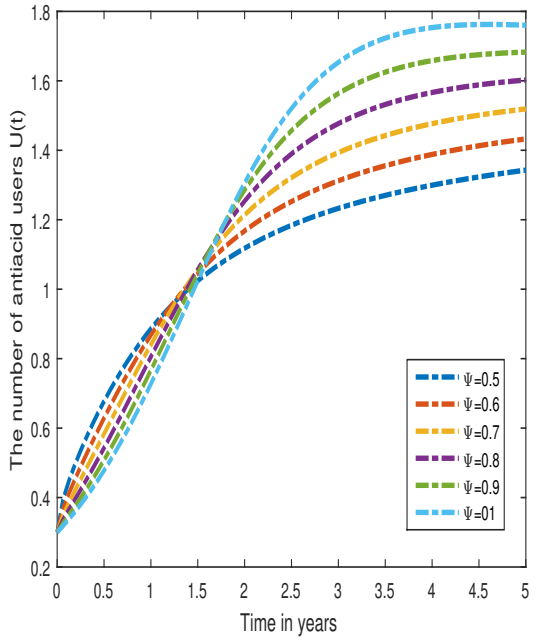

((b)) The number of antiacid users $\mathcal{U}(t)$.

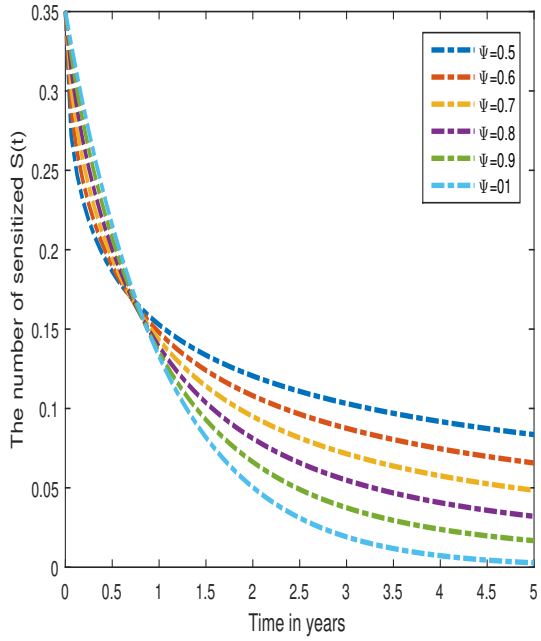

((c)) The number of sensitized $\mathcal{S}(t)$.

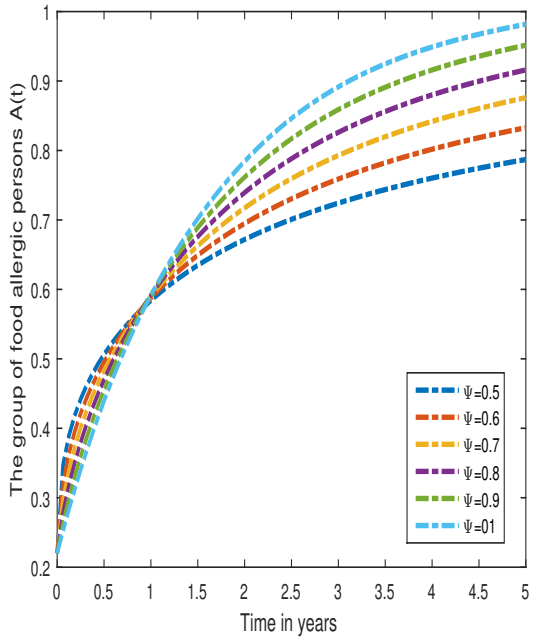

((d)) The group of food allergic persons $\mathcal{A}(t)$.

Figure 1: Paths for the solution of system (2.2) via three-step Adams-Bashforth numerical method for a long time $t = 5$ years, when $\Psi = 0.5, 0.6, 0.7, 0.8, 0.9, 01$

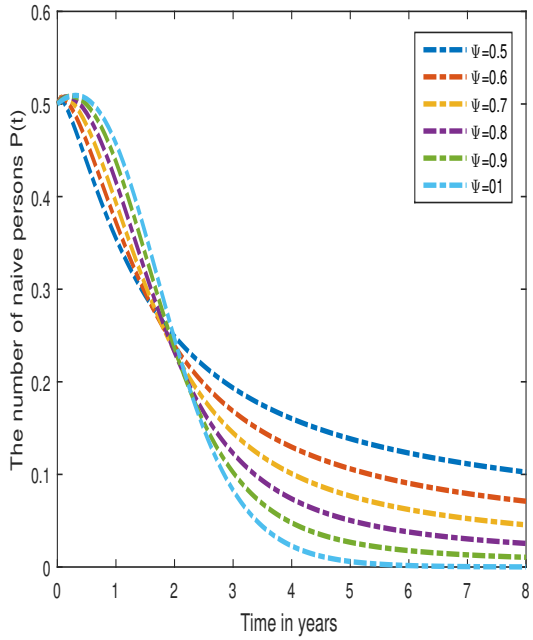

((a)) The number of naive persons $\mathcal{P}(t)$.

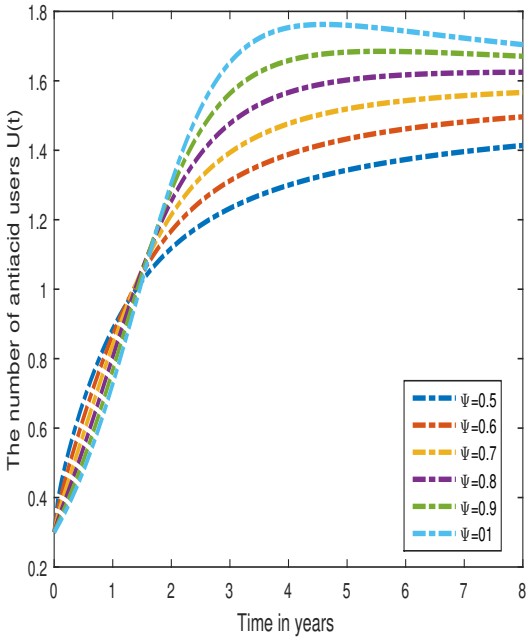

((b)) The number of antiacid users $\mathcal{U}(t)$.

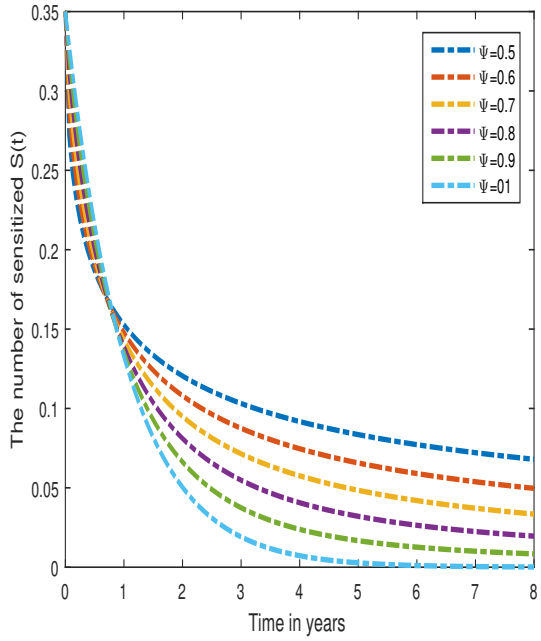

((c)) The number of sensitized $\mathcal{S}(t)$.

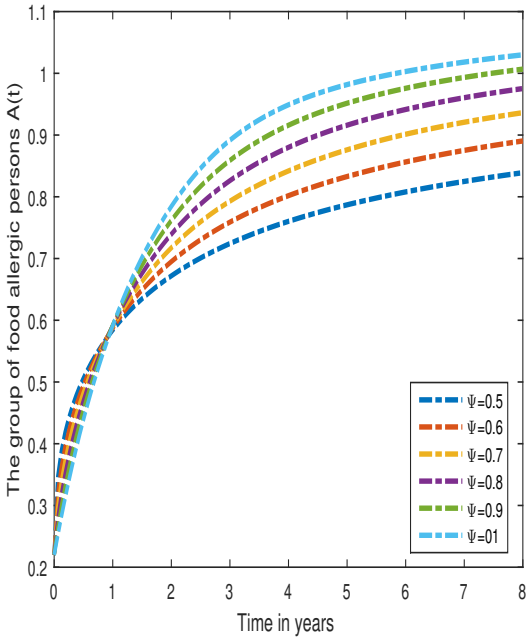

((d)) The group of food allergic persons $\mathcal{A}(t)$.

Figure 2: Paths for the solution of system (2.2) via three-step Adams-Bashforth numerical method for a long time $t = 8$ years, when $\Psi = 0.5, 0.6, 0.7, 0.8, 0.9, 01$

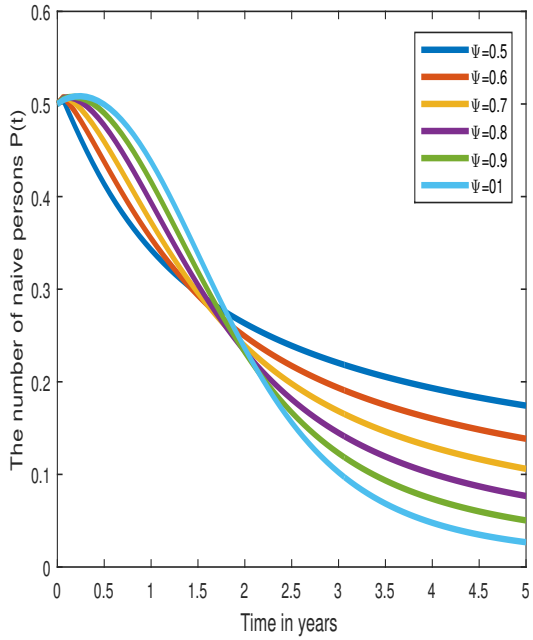

((a)) The number of naive persons $\mathcal{P}(t)$.

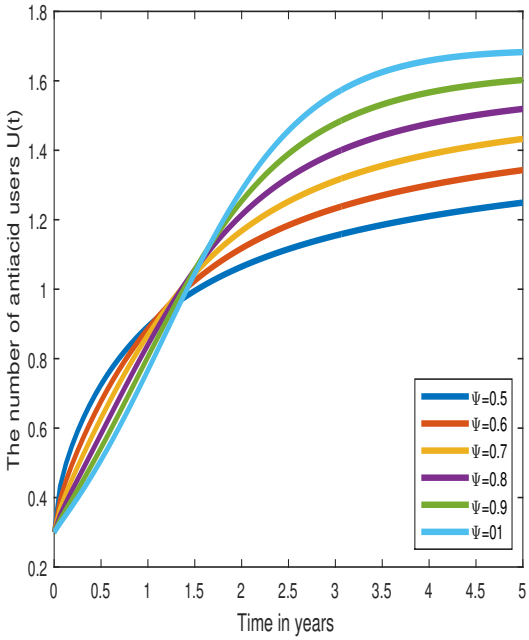

((b)) The number of antiacid users $\mathcal{U}(t)$.

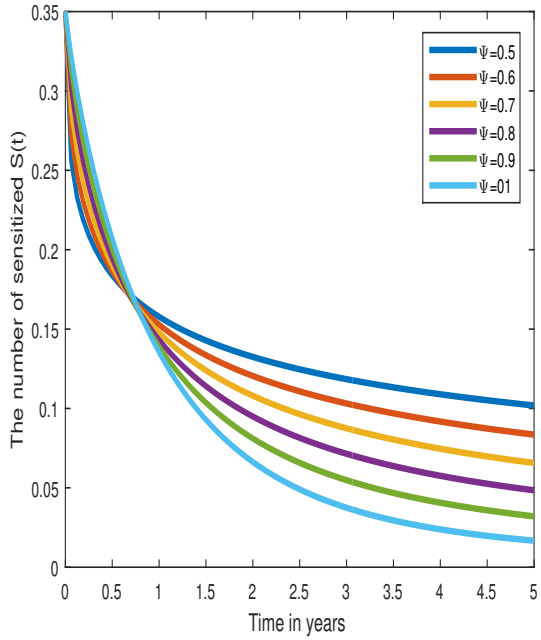

((c)) The number of sensitized $\mathcal{S}(t)$.

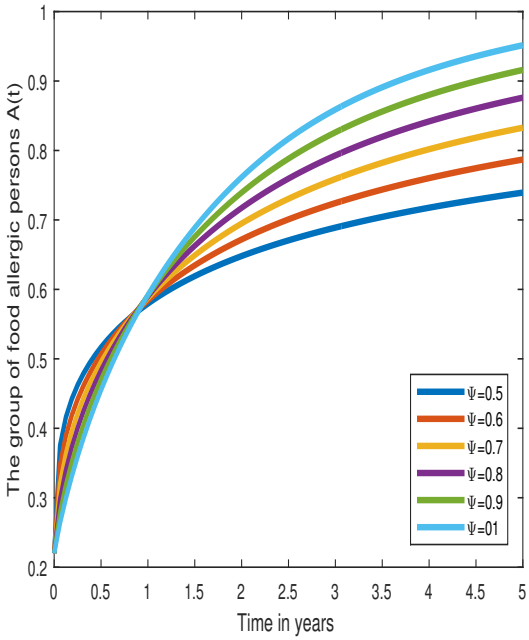

((d)) The group of food allergic persons $\mathcal{A}(t)$.

Figure 3: Paths for the solution of system (2.2) via Newton's Polynomial numerical method for a long time $t = 5$ years, when $\Psi = 0.5, 0.6, 0.7, 0.8, 0.9, 01$

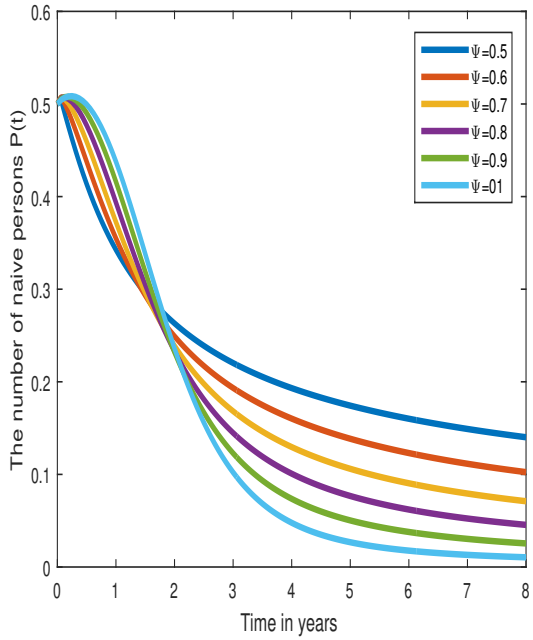

((a)) The number of naive persons $\mathcal{P}(t)$.

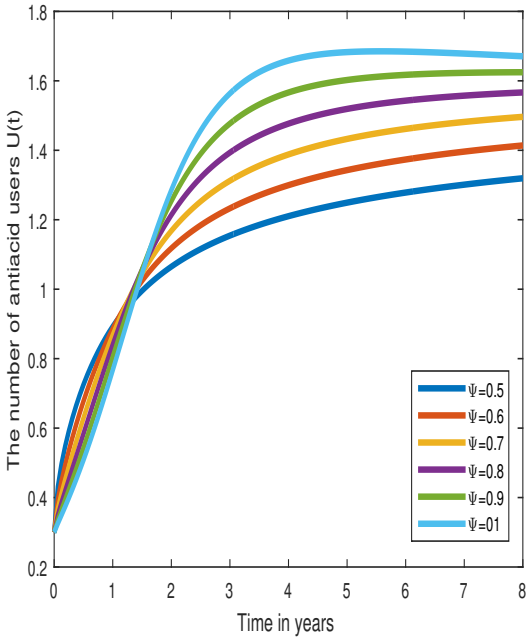

((b)) The number of antiacid users $\mathcal{U}(t)$.

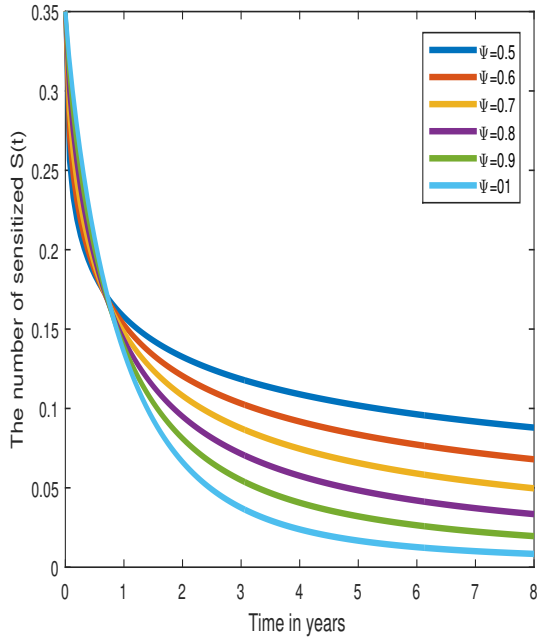

((c)) The number of sensitized $\mathcal{S}(t)$.

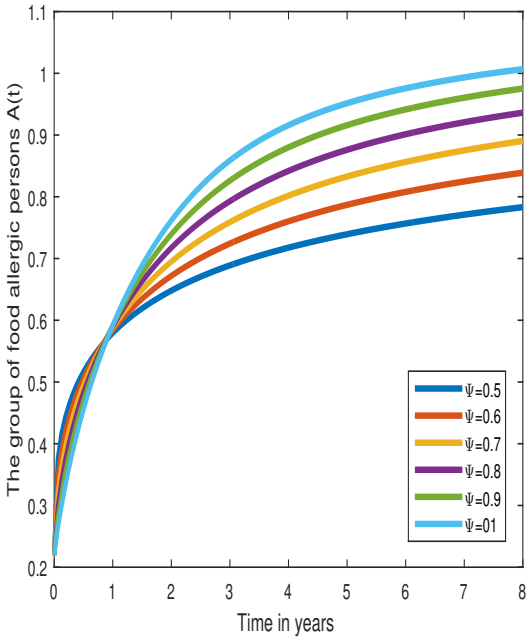

((d)) The group of food allergic persons $\mathcal{A}(t)$.

Figure 4: Paths for the solution of system (2.2) via Newton's Polynomial numerical method for a long time $t = 8$ years, when $\Psi = 0.5, 0.6, 0.7, 0.8, 0.9, 01$.

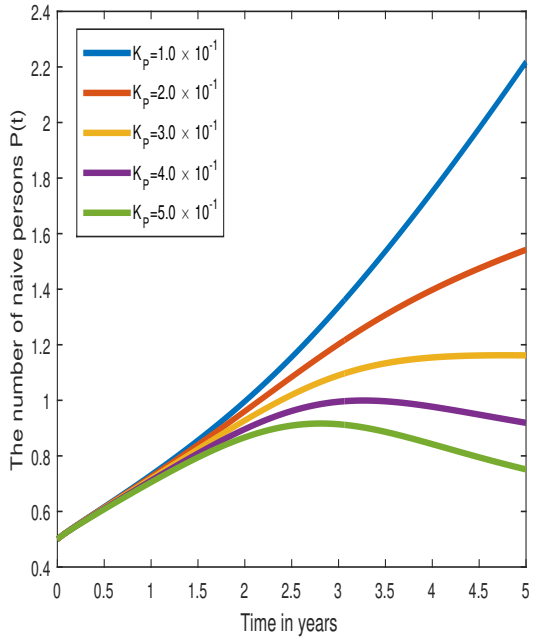

((a)) The number of naive persons $\mathcal{P}(t)$.

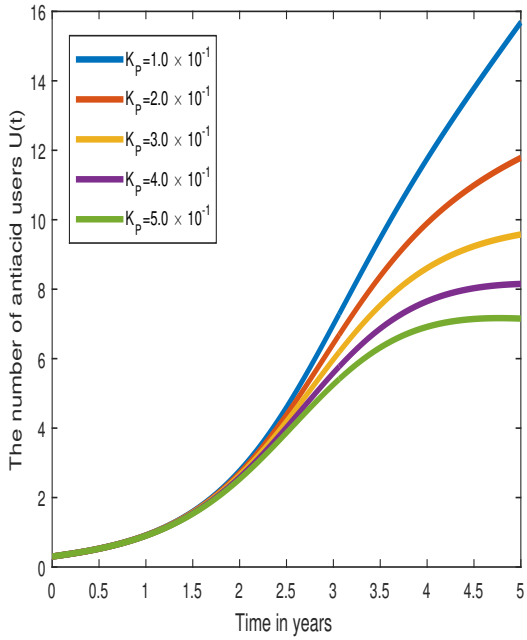

((b)) The number of antiacid users $\mathcal{U}(t)$.

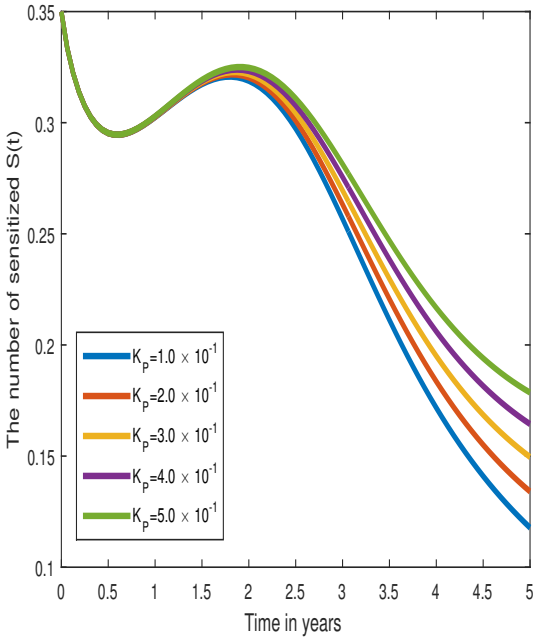

((c)) The number of sensitized $\mathcal{S}(t)$.

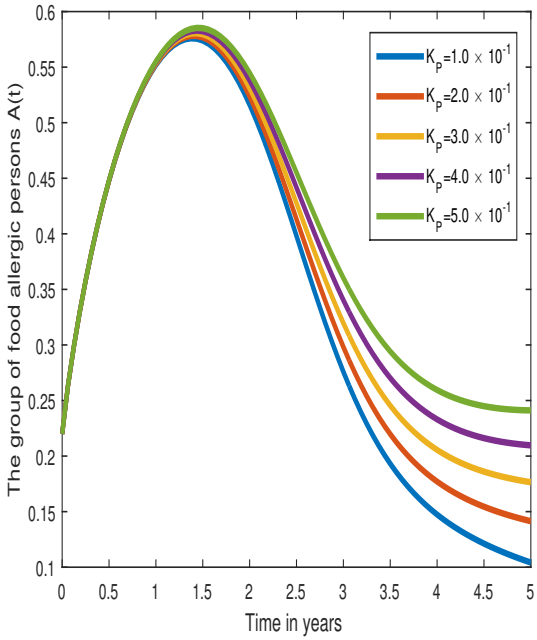

((d)) The group of food allergic persons $\mathcal{A}(t)$.

Figure 5: Impact of the parameter $\mathcal{K}_P$ which represent recruitment of antiacid users scaling factor on each state variable at fractional order $\Psi = 1$.

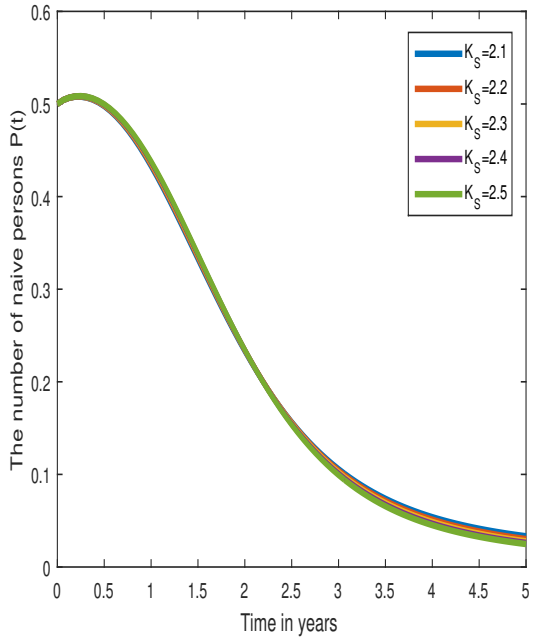

((a)) The number of naive persons $\mathcal{P}(t)$.

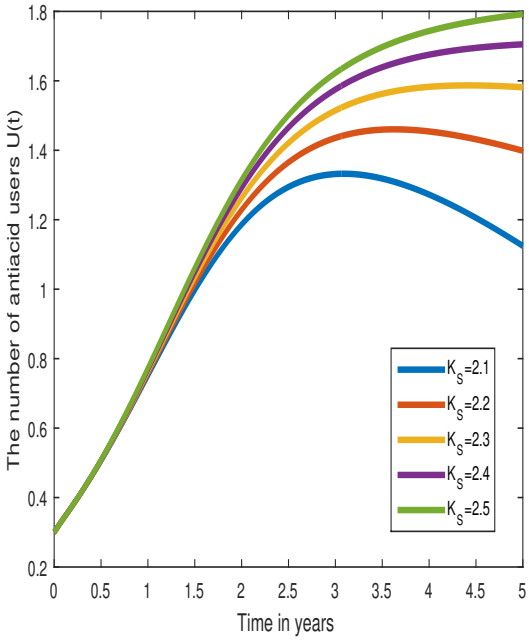

((b)) The number of antiacid users $\mathcal{U}(t)$.

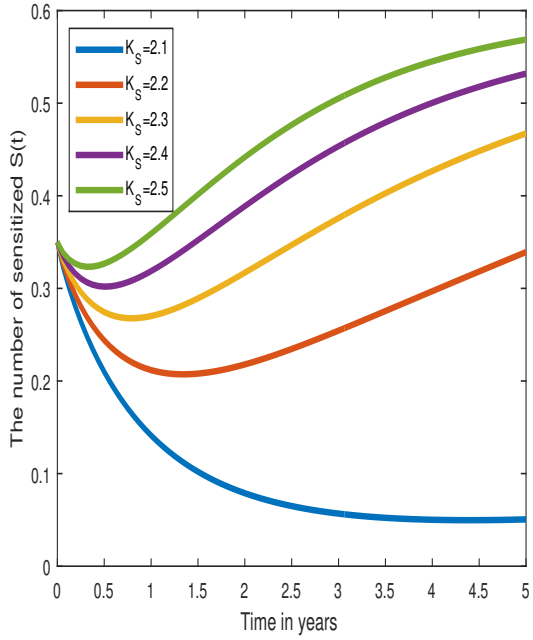

((c)) The number of sensitized $\mathcal{S}(t)$.

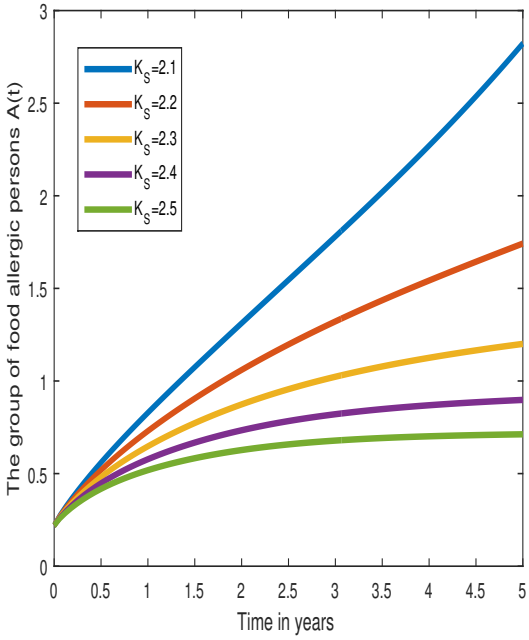

((d)) The group of food allergic persons $\mathcal{A}(t)$.

Figure 6: Impact of the parameter $\mathcal{K}_S$ which represent food allergy acquisition scaling factor on each state variable at fractional order $\Psi = 1$.

6 Conclusion

In this study, a novel mathematical model that captures the dynamics of non-integer food allergy disease is introduced. With the help of fractional calculus and ordinary differential equations (ODEs), in particular the Caputo fractional derivative operator, we aimed to fully comprehend and address the complex issues surrounding food allergy disease. Fractional calculus can be used to more accurately represent the complex dynamics governing the transmission and management of infectious diseases, such as food allergies. Our research has provided important new understandings regarding the function of the Caputo-Fabrizio fractional derivative and management techniques for the spread of food allergy disease. We investigated a fractional-order food allergy epidemic model in depth, using the Caputo-Fabrizio fractional differential operator to understand the dynamic behaviours of the system. We examined the model's long-term behaviour using a combination of qualitative analysis and computational simulations. Fixed point theory was used to establish the existence and uniqueness of the solution, and the Ulam-Hyers method was used to analyse the system's stability. We used Newton's polynomial and the three-step Adams-Bashforth numerical method as two different numerical techniques for numerical simulations. The effectiveness of the fractional order approach in capturing the complex dynamics of food allergy disease epidemics is highlighted by our findings. Additionally, these insights provide insightful advice for creating the best control strategies. Notably, our study highlights the critical value of early medical intervention in the management of food allergy disease, outlining how such interventions can result in substantial cost savings and lifesaving benefits. Additionally, we expanded our research to include a non-integer disease model for food allergies. In particular, we provided two unique numerical algorithms using various derivative operators. According to our research, the fractional model is more stable than the integer-order equivalent. This is demonstrated by the non-integer model's wider stability domain. Furthermore, we emphasise that the memory effect introduced by the fractional derivative has an inherent impact on the dynamic behaviour of our proposed model. In conclusion, our study uses fractional calculus and mathematical modelling to further our understanding of the dynamics of food allergy disease. With an emphasis on the value of early intervention and the potential advantages of the fractional order approach, the conclusions drawn from our investigations have implications for the design of efficient control strategies. This study emphasises how important it is to take into account complex dynamic systems when examining the spread and management of infectious diseases.

Author contributions

All authors has equally contributed to the preparation/drafting of this paper.

Acknowledgment

We thank anonymous referees for the suggestions that improve the paper.

Conflict of interests

This work does not have any potential conflicts of interest.

Data Availability Statement

The associated data is available upon request from the corresponding author.

Grant/Funding information

There are no funders to report for this submission.

Declaration Statement of Generative AI

The authors declare they have not used Artificial Intelligence (AI) tools in the creation of this article.

References

[1] Ibero, M., M. J. Castillo, and F. Pineda. "Allergy to cassava: a new allergenic food with cross-reactivity to latex." Journal of Investigational Allergology and Clinical Immunology 17, no. 6

(2007): 409.

[2] Galvao, C. E. S., L. K. Iwai, M. E. B. Andrade, J. Kalil, and FF Morato Castro. "Latex allergy and cross-reactivity to manioc: report of 2 cases." Journal of Allergy and Clinical Immunology 113, no. 2 (2004): S61.

[3] Gaspar, A., C. Braga, G. Pires, R. Murta, M. Morais-Almeida, and J. Rosado-Pinto. "Anaphylactic reaction to manioc: cross-reactivity to latex." (2003): 683-684.

[4] Ibero, M., M. J. Castillo, and F. Pineda. "Allergy to cassava: a new allergenic food with cross-reactivity to latex." Journal of Investigational Allergology and Clinical Immunology 17, no. 6 (2007): 409.

[5] Ishizaka, Kimishige, Teruko Ishizaka, and Margaret M. Hornbrook. "Physico-chemical properties of human reaginic antibody: IV. Presence of a unique immunoglobulin as a carrier of reaginic activity." The Journal of Immunology 97, no. 1 (1966): 75-85.

[6] Santos, K. Souza, C. Galvao, V. Resende, C. Martins, E. Vejvar, Gabriele Gadermaier, Fatima Ferreira, J. Kalil, and F. Castro. "Identification of new Brazilian allergens from manioc (Manihot esculenta)." (2011).

[7] Pali-Schöll, I., and E. Jensen-Jarolim. "Anti-acid medication as a risk factor for food allergy." Allergy 66, no. 4 (2011): 469-477.

[8] Santos, Keity Souza, Clovis Eduardo Galvao, Gabriele Gadermaier, Virginia Maria Ferreira Resende, Carlo de Oliveira Martins, Denise Shimbo Misumi, Ariana Campos Yang et al. "Allergic reactions to manioc (Manihot esculenta Crantz): Identification of novel allergens with potential involvement in latex-fruit syndrome." Journal of allergy and clinical immunology 128, no. 6 (2011): 1367-1369.

[9] Uversky, Vladimir N., Joel R. Gillespie, and Anthony L. Fink. "Why are "natively unfolded" proteins unstructured under physiologic conditions?." Proteins: structure, function, and bioinformatics 41, no. 3 (2000): 415-427.

[10] Mullin, J. M., M. C. Valenzano, M. Whitby, D. Lurie, J. D. Schmidt, V. Jain, O. Tully et al. "Esomeprazole induces upper gastrointestinal tract transmucosal permeability increase." Alimentary pharmacology therapeutics 28, no. 11-12 (2008): 1317-1325.

[11] Murray, Lisa J., Melissa Gabello, David S. Rudolph, Christopher P. Farrell, Melissa Morgan, Aaron P. Martin, James C. Underwood, M. Carmen Valenzano, and James M. Mullin. "Transmucosal gastric leak induced by proton pump inhibitors." Digestive diseases and sciences 54 (2009): 1408-1417.

[12] Khan, Amir, Rahat Zarin, Ghulam Hussain, Noor Atinah Ahmad, Mohd Hafiz Mohd, and Abdullahi Yusuf. "Stability analysis and optimal control of covid-19 with convex incidence rate in Khyber Pakhtunkhawa (Pakistan)." Results in physics 20 (2021): 103703.

[13] Zarin, Rahat. "Modeling and numerical analysis of fractional order hepatitis B virus model with harmonic mean type incidence rate." Computer Methods in Biomechanics and Biomedical Engineering 26, no. 9 (2023): 1018-1033.

[14] Khan, Amir, Rahat Zarin, Iftikhar Ahmed, Abdullahi Yusuf, and Usa Wannasingha Humphries. "Numerical and theoretical analysis of Rabies model under the harmonic mean type incidence rate." Results in Physics 29 (2021): 104652.

[15] ur Rahman, Mati, M. A. El-Shorbagy, Hussam Alrabaiah, Dumitru Baleanu, and Manuel De la Sen. "Investigating a new conservative 4-dimensional chaotic system." Results in Physics 53 (2023): 106969.

[16] Du, Shaokun, Noor Ul Haq, and Mati Ur Rahman. "Novel multiple solitons, their bifurcations and high order breathers for the novel extended Vakhnenko–Parkes equation." Results in Physics 54 (2023): 107038.

[17] Khan, Amir, Rahat Zarin, Usa Wannasingha Humphries, Ali Akgül, Anwar Saeed, and Taza Gul. "Fractional optimal control of COVID-19 pandemic model with generalized Mittag-Leffler function." Advances in difference equations 2021 (2021): 1-22.

[18] Xu, C., Tahir, S., Ansari, K.J., Rahman, M.U. and Al-Duais, F.S., 2023. On systems of fractional order differential equations for order $1 < \vartheta 2$. Fractals.

[19] Qu, Haidong, Mati ur Rahman, Shabir Ahmad, Muhammad Bilal Riaz, Muhammaad Ibrahim, and Tareq Saeed. "Investigation of fractional order bacteria dependent disease with the effects of different contact rates." Chaos, Solitons Fractals 159 (2022): 112169.

[20] Zarin, Rahat, Iftikhar Ahmed, Poom Kumam, Anwar Zeb, and Anwarud Din. "Fractional modeling and optimal control analysis of rabies virus under the convex incidence rate." Results in Physics 28 (2021): 104665.

[21] Zarin, Rahat, Amir Khan, Abdullahi Yusuf, Sayed Abdel-Khalek, and Mustafa Inc. "Analysis of fractional COVID-19 epidemic model under Caputo operator." Mathematical Methods in the Applied Sciences 46, no. 7 (2023): 7944-7964.

[22] Groß, Fridolin, Gerhard Metzner, and Ulrich Behn. "Mathematical modeling of allergy and specific immunotherapy: Th1–Th2–Treg interactions." Journal of theoretical biology 269, no. 1 (2011): 70-78.

[23] Yang, Hyun Mo, Ariana Campos Yang, Keity Souza Santos, Clovis Eduardo Galv, and Fabio Fernandes Morato Castro. "The assessment of the arising of food allergy among antiacid users using mathematical model." (2012).

[24] Yang, Hyun M. "Mathematical modeling of solid cancer growth with angiogenesis." Theoretical Biology and Medical Modelling 9, no. 1 (2012): 1-39.

[25] J. D. Murray, "Mathematical Biology," Spinger-Verlag,. N. C. Mills, P.nt in Food Allergy: Report from a New York, 1989.

[26] Madsen, Charlotte Bernhard, S. Hattersley, J. Buck, S. M. Gendel, G. F. Houben, JO'B. Hourihane, A. Mackie et al. "Approaches to risk assessment in food allergy: report from a workshop "developing a framework for assessing the risk from allergenic foods"." Food and Chemical Toxicology 47, no. 2 (2009): 480-489.

[27] Caponetto, Riccardo. Fractional order systems: modeling and control applications. Vol. 72. World Scientific, 2010.

[28] Liu, Peijiang, Anwarud Din, and Rahat Zarin. "Numerical dynamics and fractional modeling of hepatitis B virus model with non-singular and non-local kernels." Results in Physics 39 (2022): 105757.

[29] Podlubny, Igor. "An introduction to fractional derivatives, fractional differential equations, to methods of their solution and some of their applications." Math. Sci. Eng 198 (1999): 340.

[30] Caputo, Michele, and Mauro Fabrizio. "A new definition of fractional derivative without singular kernel." Progress in Fractional Differentiation & Applications 1, no. 2 (2015): 73-85.

[31] Atangana, Abdon, and Dumitru Baleanu. "New fractional derivatives with nonlocal and non-singular kernel: theory and application to heat transfer model." arXiv preprint arXiv:1602.03408 (2016).

[32] Yang, Xiao-Jun. "Fractional derivatives of constant and variable orders applied to anomalous relaxation models in heat-transfer problems." arXiv preprint arXiv:1612.03202 (2016).

[33] Podlubny, Igor. Fractional differential equations: an introduction to fractional derivatives, fractional differential equations, to methods of their solution and some of their applications. Elsevier, 1998.

[34] Caputo, Michele, and Mauro Fabrizio. "A new definition of fractional derivative without singular kernel." Progress in Fractional Differentiation & Applications 1, no. 2 (2015): 73-85.

[35] Atangana, Abdon, and Ilknur Koca. "Chaos in a simple nonlinear system with Atangana–Baleanu derivatives with fractional order." Chaos, Solitons & Fractals 89 (2016): 447-454.

[36] Kumar, Sunil, Ajay Kumar, and Mohamed Jleli. "A numerical analysis for fractional model of the spread of pests in tea plants." Numerical Methods for Partial Differential Equations 38, no. 3 (2022): 540-565.

[37] Atangana, Abdon, and Seda İğret Araz. New numerical scheme with Newton polynomial: theory, methods, and applications. Academic Press, 2021.

[38] Atangana, Abdon, and Seda İğret Araz. "Mathematical model of COVID-19 spread in Turkey and South Africa: theory, methods, and applications." Advances in Difference Equations 2020, no. 1 (2020): 1-89.

[39] Zarin, Rahat, Amir Khan, and Pushpendra Kumar. "Fractional-order dynamics of Chagas-HIV epidemic model with different fractional operators." AIMS Mathematics 7, no. 10 (2022): 18897-18924.

[40] Araz, Seda İğret. "Analysis of a Covid-19 model: optimal control, stability and simulations." Alexandria Engineering Journal 60, no. 1 (2021): 647-658.